SURFACE PROCESSES OF THE GREENLAND ICE SHEET UNDER A WARMING CLIMATE

Konrad Steffen, Liam Colgan, Nicolas Bayou, Thomas Philips
University of Colorado at Boulder
Cooperative Institute for Research in Environmental Sciences
Campus Box 216, Boulder CO 80309

NASA Grant NNX08AT85G

Progress Report
to
National Aeronautics and Space Administration, Cryospheric Program
and
National Science Foundation, Office of Polar Programs

June 2011

BASELINE SURFACE RADIATION NETWORK (BSRN) RADIOMETERS AT SUMMIT, GREENLAND

Table of Content

1. Field Expedition 2010

1.1 Logistic Summary

Date	Location	Work
April 2010		
26	Scotia-SFJ	Team members (Steffen, Colgan, McGrath, Bayou, Rial)
29	SFJ-Swiss Camp	Cargo load
30	SFJ – NASA SE	AWS download, upgrade instruments
30	NASA SE - Saddle	AWS download, upgrade instruments
30	Saddle – Dye-II-SFJ	AWS download
May 2010		
1	SFJ-DyeII-SFJ	AWS upgrade and tower extension
3	SFJ-NEEM-Thule	AWS download
4-6	Thule	Bad weather days
7	Thule-NEEM-Humboldt	AWS download
7	Humboldt-Petermann	AWS repair
8	Petermann-GITS	AWS upgrade
8	GITS-NEEM-NGRIP	Download NGRP and remove station
8	NGRIP-SFJ	End of AWS traverse
9	SFJ – Swiss Camp.	Put-in (Steffen, Colgan, McGrath, Zwally)
9	SC – Up50-CP1-SFJ	GPS download, AWS download and extension
9	SC– CP1 – SC-SFJ	Cargo put-in (Rial, Bayou)
10	SC (Swiss Camp)	AWS download, GPS download
11	JAR1,	AWS download, GPS download
13	SC-Moulin-SC	AWS download
14	SC-JAR2-SC	AWS download, GPS download and removal
15	S16	GPS download, AWS download
15	SC	Pressure sensor installment for lake
15	SC	Zwally leaves by helicopter to Ilulissat
16	Up18	New GPS site installment
17	SC	Snow and ablation survey
18	SC-Ilulissat	Helicopter to Ilulissat (Steffen,Colgan,McGrath, Bayou,Rial)
20	Ilulissat-SFJ	Relocation team to Kangerlussuaq
21	SFJ-US	Team members Steffen, Colgan, McGrath, Bayou, Rial
August 2010		
12	US-SFJ	Team Bayou, Pottinger to Greenland
12	CPH-SFJ	Team Schroff, Frei to Greenland from Switzerland

13	SFJ-Summit	Team Bayou, Pottinger, Schroff, Frei to Summit
14	Summit	AWS download, tower extension
15	Summit	BSRN tower extension and upgrade
16	Summit	Borehole thermistor removal (Moto's project)
17-19	Summit	50 m tower upgrade
20	Summit-SFJ	Team Steffen and Schroff return to Kanger
22	SFJ-CPH	Team Schroff and Frei
22	SFJ-US	Team Bayou, Pottinger

1.2 Automatic Weather Station Maintenance

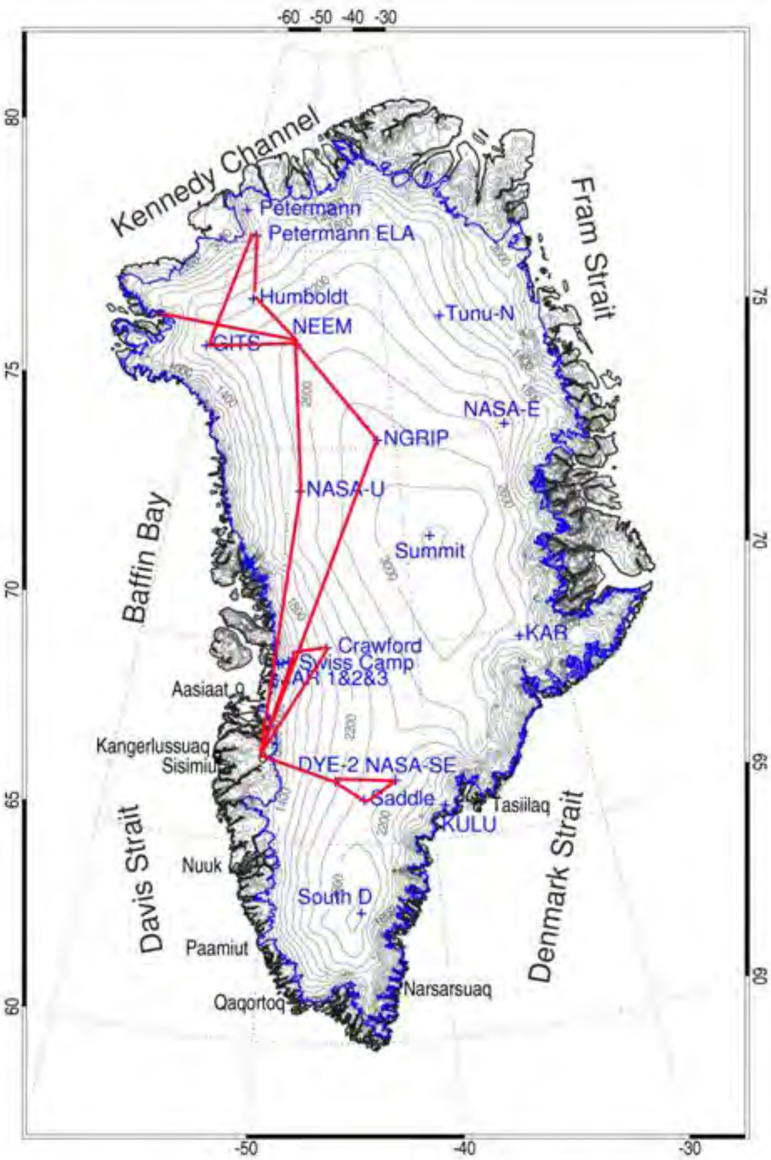

Figure 1.1: Greenland Climate Network (GC-Net) automatic weather stations as of summer 2010. The red arrows indicate the Twin Otter flight path for the AWS maintenance described in the logistic summary.

1.3 Personal

Name	**Institution**	**Arr.**	**Dep.**
AWS support, Swiss Camp research, Summit station			
Konrad Steffen	CU-Boulder	4/26	5/21
William Colgan	CU-Boulder	4/26	5/21
Dan McGrath	CU-Boulder	4/26	5/21
Nicolas Bayou	CU-Boulder	4/26	5/21
Jay Zwally	NASA-GSFC	4/27	5/15
Jose Rial	Univ. NC	4/26	5/21
Nicolas Bayou	CU-Boulder	8/12	8/22
Jim Pottinger	PolarTech	8/12	8/22
Karl Schroff	ETH-Zürich	8/12	8/22
H.J. Frei	ETH-Zürich	8/12	8/22

2. The Greenland Climate Network (GC-Net)

2.1 Overview

The GC-Net currently consists of 17 automatic weather stations distributed over the entire Greenland ice sheet (Figure 1.1). Four stations are located along the crest of the ice sheet (2500 to 3200 m elevation range) in a north-south direction, eight stations are located close to the 2000 m contour line (1830 m to 2500 m), and three stations are positioned in the ablation region (50 m to 800 m), and two stations are located at the equilibrium line altitude at the west coast and in the north.

The GC-Net was established in spring 1990 with the intention of monitoring climatological and glaciological parameters at various locations on the ice sheet over a time period to assess the climate and its variability. The first AWS was installed in 1990 at the Swiss Camp, followed by four AWS in 1995, four in 1996, five in 1997, another four in 1999, one in 2002 one in 2003, and the latest one at NEEM in support for the new deep ice core in 2006. Our objectives for the Greenland weather station (AWS) network are to measure daily, annual and interannual variability in accumulation rate, surface climatology and surface energy balance at selected locations on the ice sheet, and to measure near-surface snow density at the AWS locations for the assessment of snow densification, accumulation, and metamorphosis.

In addition to providing climatological and glaciological observations from the field, further application of the GC-Net data include: the study of the ice sheet melt extent (*Abdalati and Steffen,* 2001); estimates of the ice sheet sublimation rate (*Box and Steffen*, 2001); reconstruction of long-term air temperature time series (*Shuman at al.,* 2001), assessment of surface climate (*Steffen and Box*, 2001), and the interpretation of satellite-derived melt features of the ice sheet (*Nghiem et al.,* 2001). Potential applications for the use of the GC-Net data are: comparison of in-situ and satellite-derived surface parameters, operational weather forecast; validation of climate models; and logistic support for ice camps and Thule AFB.

Since summer 2010, the GC-Net data is transmitted hourly to the Danish Meteorological Institute (DMI) and used for weather forecast. All GC-Net stations have been assigned a WMO code number; hence the data is available worldwide on an hourly basis for weather prediction models.

2.2 Data Processing Tools

The last year has been dedicated to redesign the existing Greenland Climate Network (*GC-Net*) data processing tools. We dedicated our time to create a set of new tools written in MATLAB which are portable on Unix and Window platforms, insuring fast and reliable data processing.

2.3 Transmitted Data

With satellite transmitters (*GOES* & *Argos*), the Automated Weather Stations (AWS) constituting the Greenland Climate Network transmit every hour a given set of weather parameters. This valuable dataset is made available to the scientific community on *CIRES* web site (http://cires.colorado.edu/steffen/gcnet/). The main parameters (atmospheric pressure, air temperatures, wind velocity and direction, incoming and reflected short wave radiations) are displayed as plots, when the whole dataset is available upon request. Starting in summer 2010, the *GC-Net* data is transmitted hourly to the *Danish Meteorological Institute* (*DMI*) for their weather models calibration.

The *GC-Net* data is transmitted by two different satellite types depending on the station's latitude (*Argos* for the northernmost stations, *GOES* satellites otherwise), using different transmission protocols. Every hour, the data is downloaded from *Argos* and *GOES* servers and decoded. At this stage of the process, we are able to calibrate the data, but also to correct errors that may have occurred while servicing the *AWS* (orientation, datalogger date and time). Once calibrated and corrected, the data is cleaned (corrupt values are removed) and added to the previously processed data file that is available to display on the web site. *Figure 2.1* shows a schematic of the process.

The whole process is automated and does not require human intervention. Each *AWS* has a set of files defining its specificities (calibration, corrections, limits). After a station has been serviced, these files are updated.

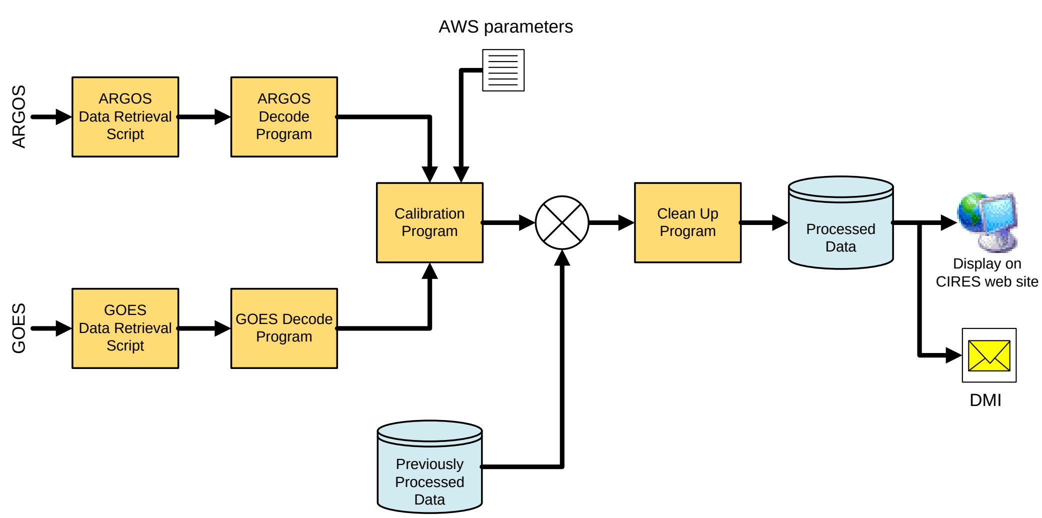

Figure 2. 1: Transmitted AWS data process

2.4 Downloaded Data

When an *AWS* is serviced, the data logger is downloaded and the resulting dataset needs to be processed before being available to the scientific community. Two different tools to process the dataset have been developed. These tools are Graphic User Interface (*GUI*) based for total user control.

- *ShapeRAW* reads the raw file downloaded from the data logger. The user can browse and define the different channels which are plotted. The channels sequence is saved for reference. The A Level file is then created. It is the raw data in the correct channels sequence. *Figure 2.2* shows the *ShapeRAW* interface.

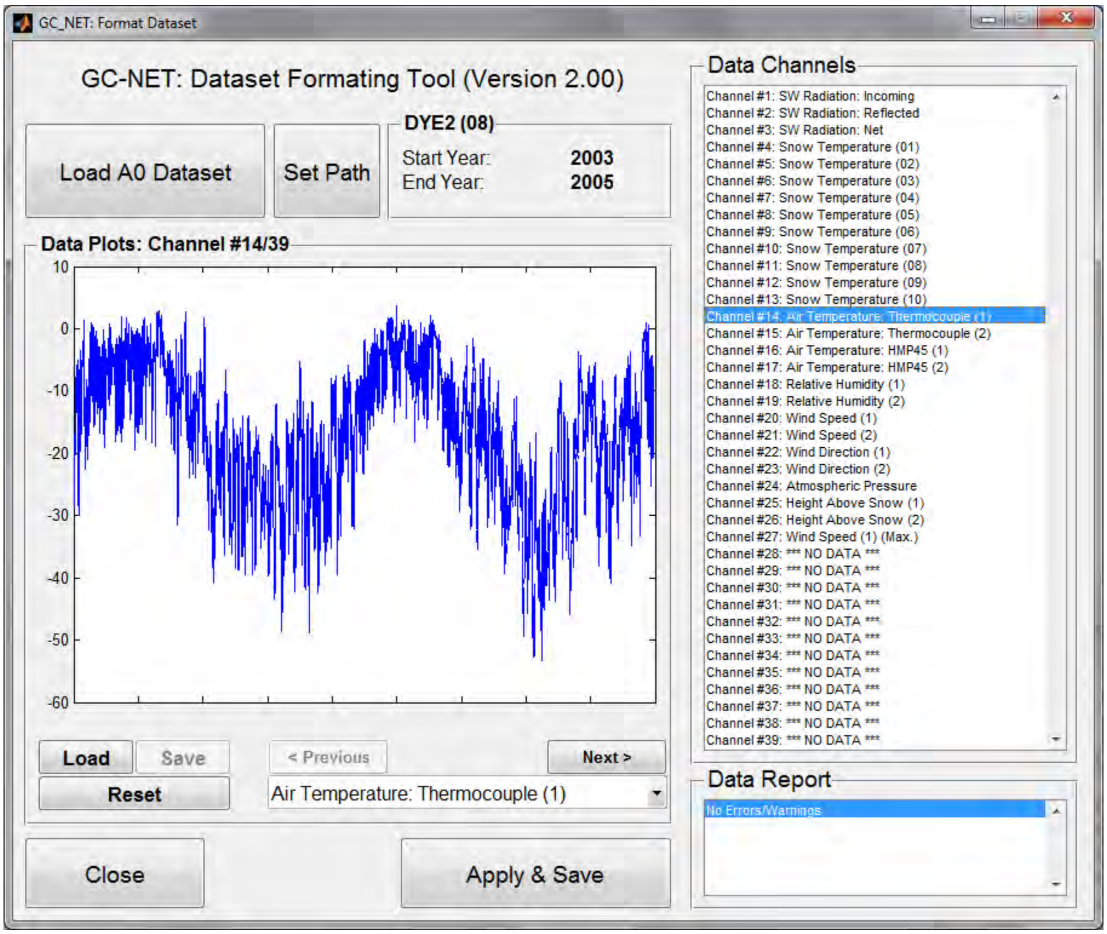

Figure 2.2: ShapeRAW interface.

- *Quality Check* reads the previous standard format file (*A Level*). Because the *A Level* file is the raw dataset with a standard channels sequence, the user has to calibrate the data and define the AWS instruments set up (distances between instruments for additional calculations). Limits can also be defined. Once calibrated, the different channels can be cleaned. The cleaning part of the process consists in removing unwanted data. The user draws boxes around the data to be removed. These boxes, or filters, can be saved for reference, process replication or future modifications. Once cleaned, additional parameters are computed based on the cleaned dataset (2 and 10 meters wind velocities, Zenith angle, albedo). The resulting dataset (*C Level*) is added to the database. When a specific period is reprocessed, the database is updated. *Quality Check* also allows us to process and add the transmitted data to the database. *Figure 2.3* shows the *Quality Check* interface.

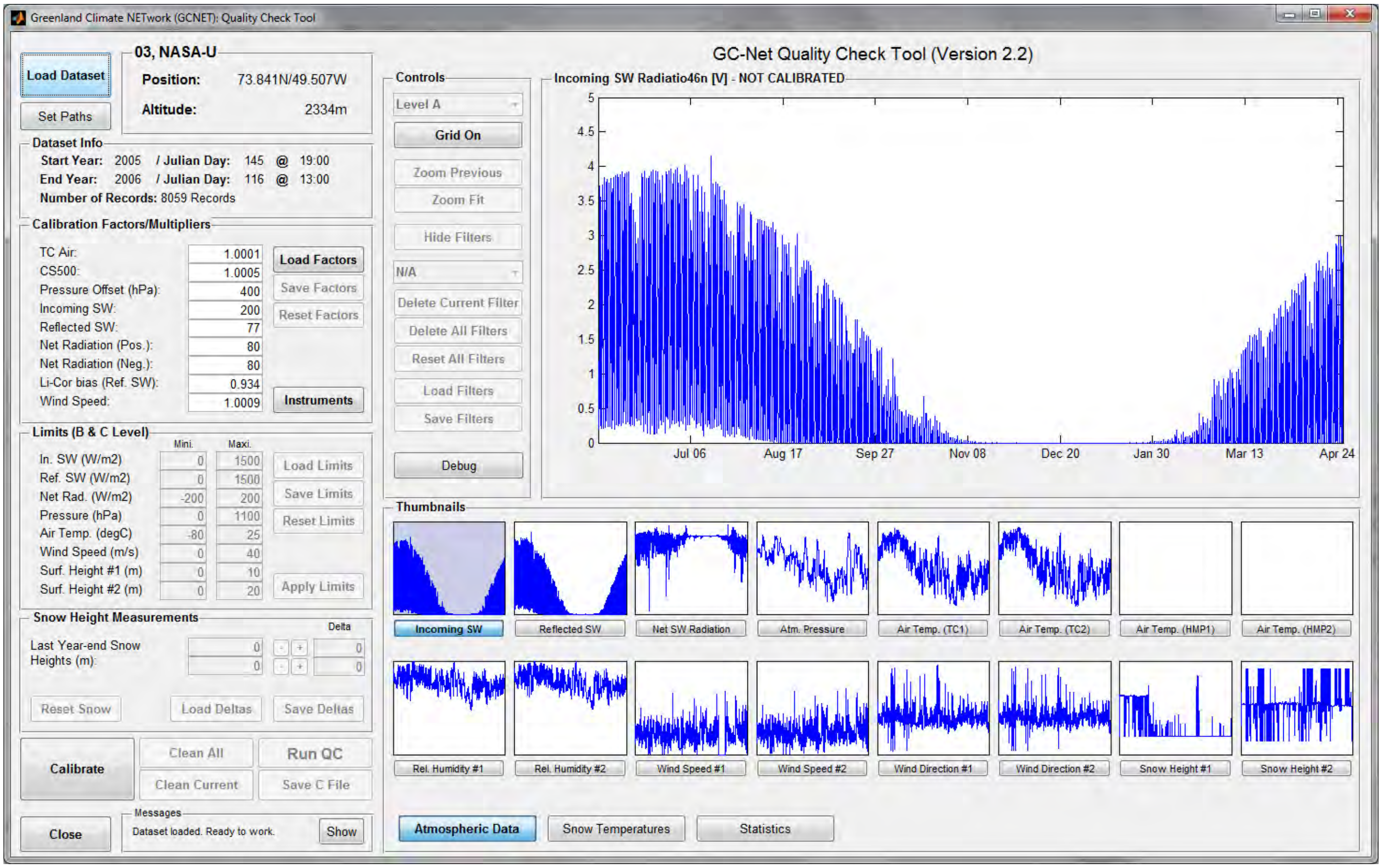

Figure 2.3: QualityCheck interface.

These two tools have been developed with the idea that, at any time, the process chould be replicated. Every parameter of the process, from the calibration factors to the cleaning filters, are saved and can be reused or modified in the future. This allows us to assure the quality of the *GC-Net* dataset.

2.5 GC-Net Users

The GC-Net data request from the beginning of 2010 to present (20 June 2011) registered 248 user request (Table 2.1). The web interface allows us to capture the email and affiliation of all GC-Net users, including a short description of their use of the Greenland Climate data. The data request is processed on a UNIX 4-processor workstation and the data is transferred on a FTP site for direct downloading. We will continue to maintain the main portal for all GC-Net data distribution, the main raison being the frequent data reprocessing to increase data quality. The data request has increased by approximately 100% since our previous progress report in April 2010.

No.	Email	Name	Organization	Approved
431	sjsk@nsidc.org	Siri Jodha KHALSA	NSIDC	01-06-10
432	malin.johansson@natgeo.su.se	Malin Johansson	Stockholm University	01-08-10
433	david.podrasky@gi.alaska.edu	David Podrasky	Univ. of Alaska Geophysical Institute	01-16-10
434	lwang2@gmu.edu	Lingli Wang	Geroge Mason University	01-16-10
435	ernsdorf@uni-trier.de	Thomas Ernsdorf	University of Trier, Fac. of Geography/Geosciences, Dept. of Environmental Meteorology	02-05-10
436	chad.steed@nrlssc.navy.mil	Chad Steed	Naval Research Laboratory	02-06-10

437	yjz630@163.com	yjz	Jinan university, China	02-06-10	
438	yjz630@sina.com	Jianzhang Yu	Jinan University	02-10-10	
439	thomas.nagler@enveo.at	Thomas Nagler	Univ Innsbruck / ENVEO	02-13-10	
440	lisa.ho@colorado.edu	lisa ho	CIRES	12-08-10	
441	crb50@cam.ac.uk	Catherine Baggs	Scott Polar Research Institute	02-18-10	
442	liamdmathdude@hotmail.com	Russell	High-school project	02-18-10	
443	liamdmathdude@hotmail.com	Russell	High-school project	02-20-10	
444	limaruss@sympatico.ca	Maria	High-school project	02-20-10	
445	liamdmathdude@hotmail.com	Russell	High-school project	02-22-10	
446	cpchen@asiaa.sinica.edu.tw	Ben chen	Academia Sinica Inst. of Astronomy and Astrophysics	02-24-10	
447	adasgupt@uncc.edu	Aritra Dasgupta	University of North Carolina at Charlotte	02-24-10	
448	xiaolei@atmos.umd.edu	XIAOLEI NIU	University of Maryland,College Park, Maryalnd,USA	02-24-10	
449	xiaolei@atmos.umd.edu	XIAOLEI NIU	University of Maryland	02-25-10	
450	m.a.brandon@open.ac.uk	Mark Brandon	The Open University	02-25-10	
451	xiaolei@atmos.umd.edu	XIAOLEI NIU	University of Maryland,College Park, Maryalnd,USA	03-01-10	
452	adasgupt@uncc.edu	Aritra Dasgupta	University of North Carolina at Charlotte	03-01-10	
453	bfm@dartmouth.edu	Blaine Morriss	Dartmouth College	03-10-10	
454	beal@dartmouth.edu	Sam Beal	Dartmouth College	03-04-10	
455	A.J.S.Farrar@sms.ed.ac.uk	Andrew Farrar	University of Edinburgh	03-06-10	
457	pierre08250@msn.com	Huat	University	03-10-10	
458	mlupker@crpg-cnrs.nancy.fr	Maarten Lupker	CRPG-CNRS FRANCE	03-21-10	
459	lwang2@gmu.edu	Lingli Wang	George Mason University	03-23-10	
460	matthew.hoffman@nasa.gov	Matthew J. Hoffman	NASA Goddard Space Flight Center	03-27-10	
461	jplieberman@gmail.com	Jordan Lieberman	University of Georgia Climate Research Lab	05-04-10	
462	khalid.hussein@colorado.edu	Khalid Hussein	ESOC, CIRES	03-31-10	
463	liamdmathdude@hotmail.com	Russell	High-school project	04-12-10	
464	ddwang@umd.edu	Dongdong Wang	University of Maryland	04-12-10	
465	khalid.hussein@colorado.edu	Khalid Hussein	ESOC, CIRES	04-12-10	
466	mira.schmidt@hotmail.de	Schmidt	Technical University Braunschweig	04-13-10	
467	lwang2@gmu.edu	Lingli Wang	GMU	04-13-10	
468	brandt@atmos.washington.edu	Richard Brandt	University of Washington Dept. of Atm. Sciences	04-14-10	
469	khalid.hussein@colorado.edu	Khalid Hussein	ESOC, CIRES	04-14-10	
470	princesss1085@yahoo.com	Lauren Ingram	Wenatchee Valley College at Omak	04-21-10	
471	mernild@lanl.gov	Sebastian H. Mernild	LANL	04-21-10	
472	mernild@lanl.gov	Sebastian H. Mernild	LANL	04-23-10	
473	Thomas.Phillips@colorado.edu	Thomas Phillips	University of Colorado	04-23-10	
474	rollo@reidsteel.co.uk	R Reid	Reidsteel	04-27-10	
475	bailesheng@hotmail.com	Lesheng Bai	Byrd Polar Research Center, The Ohio State Univ.	05-02-10	
476	georgette_holmes@hotmail.com	Georgette Holmes	George Mason University	05-02-10	
477	afb39@cam.ac.uk	Alison Banwell	Scott Polar Research Institute, Univ. of Cambridge	05-12-10	
478	aorsi@ucsd.edu	Anais Orsi	Scripps Inst of Oceanography	05-13-10	
479	ehanna@sheffield.ac.uk	Edward Hanna	University of Sheffield	05-19-10	
481	djl22@psu.edu	Derrick	Pennsylvania State	05-31-10	
482	todd.martin@amec.com	Todd Martin	AMEC Earth & Environmental	05-31-10	
483	jonathan.day@bris.ac.uk	Jonathan Day	University of Bristol	06-01-10	
485	konrad.steffen@colorado.edu	koni	CIRES	06-01-10	
486	djl22@psu.edu	Derrick J Lampkin	Pennsylvania State University	06-01-10	
488	burkett@essc.psu.edu	Peter Burkett	Pennsylvania State University	06-07-10	
489	wuhaorangeo@gmail.com	Haoran Wu	Beijing Normal University, China	06-12-10	
490	wlz1220@sina.com	Wang LiZhao	Beijing Normal University	06-12-10	

491	wuhaorangeo@gmail.com	Haoran Wu	Beijing Normal University, China	06-12-10	
492	ehanna@sheffield.ac.uk	Edward Hanna	Reader in Climate Change	06-13-10	
493	lisa.ho@colorado.edu	Lisa Ho	CIRES	06-16-10	
494	lisa.ho@colorado.edu	Lisa Ho	CIRES/CU	12-08-10	
495	florian.figwer@gmail.com	Figwer Florian	University Innsbruck	06-16-10	
496	florian.figwer@gmail.com	Figwer Florian	University Innsbruck	06-16-10	
497	florian.figwer@gmail.com	Figwer Florian	University Innsbruck	06-16-10	
498	jack.saba@nasa.gov	jack Saba	Code 614.1, NASA/GODDARD	06-24-10	
499	dva@geus.dk	Dirk van As	GEUS	06-25-10	
500	jplieberman@gmail.com	Jordan Lieberman	University of Georgia Climate Research Lab	06-28-10	
501	florian.figwer@gmail.com	Figwer Florian	University Innsbruck	06-30-10	
503	anbh@uaa.alaska.edu	Birgit Hagedorn	University o Alaska Anchorage	07-08-10	
504	eeaal@leeds.ac.uk	amber Leeson	University of Leeds	07-06-10	
505	heather.trantham@tetratech.com	Heather Trantham	Tetra Tech	07-08-10	
506	jdv150@psu.edu	Justin VanderBerg	Penn State University	07-10-10	
507	jonathan.day@bris.ac.uk	Jonathan Day	University of Bristol	07-13-10	
508	robert_w_bowne@raytheon.com	Bob Bowne	Raytheon	07-17-10	
509	quidnet@sbcglobal.net	John Heffernan	Local Weather Club and World Meteor. Monitoring	07-19-10	
510	jdv150@psu.edu	Justin VanderBerg	Penn State University	07-19-10	
511	twilap@u.washington.edu	Twila Moon	University of Washington	07-21-10	
512	twilap@u.washington.edu	Twila Moon	University of Washington	07-21-10	
513	jack.saba@nasa.gov	jack saba	nasa/gsfc	07-21-10	
514	santiago.delapena@ed.ac.uk	Santiago de la Peña	University of Edinburgh	07-21-10	
515	jdv150@psu.edu	Justin VanderBerg	Penn State University	07-22-10	
516	wind_00172@msn.com	sheng gui	UMD	07-26-10	
517	santiago.delapena@ed.ac.uk	Santiago de la Peña	University of Edinburgh	07-26-10	
518	santiago.delapena@ed.ac.uk	Santiago de la Peña	University of Edinburgh	07-26-10	
519	matthew.shupe@colorado.edu	Matthew Shupe	CIRES	07-27-10	
520	daniel.mcgrath@colorado.edu	Dan McGrath	CIRES	07-28-10	
521	santiago.delapena@ed.ac.uk	Santiago de la Peña	University of Edinburgh	07-29-10	
522	eeaal@leeds.ac.uk	amber Leeson	University of Leeds	07-30-10	
523	mjw272@cornell.edu	Mike Willis	Cornell University	08-03-10	
524	lanini@slf.ch	Fabienne Lanini	Institute for Snow and Avalanche Research SLF	08-04-10	
525	pwooley@bowdoin.edu	Pablo Wooley	University of Chicago	08-04-10	
526	kirill.khvorostovsky@nersc.no	Kirill	Khvorostovsky	08-05-10	
527	pwooley@bowdoin.edu	Pablo Wooley	University of Chicago	08-06-10	
528	santiago.delapena@ed.ac.uk	Santiago de la Peña	University of Edinburgh	08-09-10	
529	santiago.delapena@ed.ac.uk	Santiago de la Peña	University of Edinburgh	08-09-10	
530	santiago.delapena@ed.ac.uk	Santiago de la Peña	University of Edinburgh	08-09-10	
532	plummer@ku.edu	Joel Plummer	CReSIS	08-16-10	
534	mewo2@cam.ac.uk	Martin O Leary	Scott Polar Research Institute	08-18-10	
535	pditlev@nbi.ku.dk	Peter Ditlevsen	Centre for Ice and Climate	08-27-10	
536	sbs@gfy.ku.dk	Sebastian B. Simonsen	Centre for Ice and Climate, NBI	08-27-10	
537	plp@dmi.dk	Philippe Lucas-Picher	Danish Meteorological Institute	08-26-10	
538	florian.mueller@uibk.ac.at	Florian Mueller	University of Innsbruck	08-27-10	
539	675151152@qq.com	Unkown	unknown	09-01-10	
541	gwk.moore@utoronto.ca	Kent Moore	University of Toronto	09-04-10	
542	r.morris@abdn.ac.uk	Richard Morris	University of Aberdeen, Aberdeen, UK	09-06-10	
543	hanschr@gfy.ku.dk	Hans Christian Steen	Centre for Ice and Climate, NBI	09-06-10	
544	dva@geus.dk	Dirk van As	Geological Survey of Denmark and Greenland	09-09-10	

545	lwake@ucalgary.ca	L Wake	University of Calgary	09-17-10	
546	daniel.mcgrath@colorado.edu	Daniel McGrath	CIRES	09-17-10	
547	yu-li.liang@colorado.edu	Yuli Liang	Computer Science, CU Boulder.	09-20-10	
548	soroushr@buffalo.edu	Soroush	University at Buffalo Remote Sensing LAB	09-27-10	
549	dreusch@ees.nmt.edu	David Reusch	New Mexico Tech	10-14-10	
550	r.morris@abdn.ac.uk	Richard Morris	University of Aberdeen, Aberdeen, UK	10-04-10	
551	xianweiw@uci.edu	xianwei wang	University of California Irvine	03-03-11	
552	hwiebe@uni-bremen.de	Heidrun Wiebe	Institute for Environmental Physics	03-03-11	
554	xuanbing_qy@163.com	Ying Qu	Beijing Normal University	10-13-10	
555	soroushr@buffalo.edu	Soroush	University at Buffalo Remote Sensing LAB	10-13-10	
558	xiaolei@atmos.umd.edu	XIAOLEI NIU	University of Maryland,College Park, Maryalnd,USA	10-15-10	
559	thomas.jackson@earth.ox.ac.uk	Thomas Jackson	Oxford University	10-15-10	
560	xiaolei@atmos.umd.edu	XIAOLEI NIU	University of Maryland,College Park, Maryalnd,USA	10-15-10	
561	xiaolei@atmos.umd.edu	XIAOLEI NIU	University of Maryland,College Park, Maryalnd,USA	10-15-10	
562	xiaolei@atmos.umd.edu	XIAOLEI NIU	University of Maryland,College Park, Maryalnd,USA	10-15-10	
563	r.morris@abdn.ac.uk	Richard Morris	University of Aberdeen, Aberdeen, UK	10-18-10	
564	kh8378@bristol.ac.uk	Katy Hargreaves	University of Bristol	10-24-10	
565	abcorbet@uvm.edu	Lee Corbett	University of Vermont Department of Geology	10-24-10	
566	lapres@gci.net	David Lappi	LAPP Resources, Inc.	10-26-10	
567	jeff.ridley@metoffice.gov.uk	Jeff Ridley	UK Met Office, Hadley Centre	10-26-10	
568	dva@geus.dk	Dirk van As	GEUS	10-28-10	
569	clandow1@uwyo.edu	Claire Landowski	University of Wyoming	11-01-10	
570	clhaman@mail.uh.edu	christine haman	university of houston	11-01-10	
571	vasfas_aua@yahoo.com	Vassilia	Fassouli	11-03-10	
573	mernild@lanl.gov	Sebastian Mernild	Los Alamos Natl. Lab	11-03-10	
574	mernild@lanl.gov	Sebastian Mernild	Los Alamos Natl. Lab	11-04-10	
575	mernild@lanl.gov	Sebastian Mernild	Los Alamos Natl. Lab	11-04-10	
576	matthias.reif@student.uibk.ac.at	Reif Matthias	University of Innsbruck	11-08-10	
577	ccox20@uwyo.edu	Christopher Cox	University of Wyoming Dept. Geol. and Geophysics	11-08-10	
578	jdv150@psu.edu	Justin VanderBerg	Penn State University	11-14-10	
579	matthias.reif@student.uibk.ac.at	Reif Matthias	University of Innsbruck	11-14-10	
581	aboldova@gmail.com	Albena	TU München	11-14-10	
584	dellagiu@gi.alaska.edu	Daniella DellaGiustina	Geophysical Institute, University of Alaska, Fairbanks	11-17-10	
586	santiago.delapena@ed.ac.uk	Santiago de la Peña	University of Edinburgh	11-26-10	
587	santiago.delapena@ed.ac.uk	Santiago de la Peña	University of Edinburgh	11-26-10	
588	konrad.steffen@colorado.edu	Koni steffen	CIRES	11-24-10	
596	cheng1986h@163.com	chenhui	uestc	12-06-10	
597	ernsdorf@uni-trier.de	Thomas Ernsdorf	University of Trier, Fac. of Geography/Geosciences,	12-06-10	
598	ernsdorf@uni-trier.de	Thomas Ernsdorf	University of Trier, Fac. of Geography/Geosciences,	12-08-10	
599	thomas.jackson@earth.ox.ac.uk	Thomas Jackson	Oxford University	12-08-10	
600	lisa.ho@colorado.edu	Lisa test	Oxford University	12-08-10	
601	robert.l.hawley@dartmouth.edu	Bob Hawley	Dartmouth College	12-09-10	
602	mail@mjochner.com	Matthias Jochner	Universität Erlangen-Nürnberg	12-09-10	
604	afb39@cam.ac.uk	Alison Banwell	Scott Polar Research Institute, Univ. of Cambridge	2-22-10	
605	russell.layberry@ouce.ox.ac.uk	russ	oxford university	01-03-11	
606	afb39@cam.ac.uk	Alison Banwell	Scott Polar Research Institute	01-11-11	
607	ggp08jmc@shef.ac.uk	Joseph Cook	University of Sheffield	01-14-11	
608	aku.riihela@fmi.fi	Aku Riihelä	Finnish Meteorological Institute	01-20-11	
609	tlgontheicce@hotmail.com	Terrance Gacke	contract ice core driller with IDDO - Madison Wisc.	01-20-11	
610	afb39@cam.ac.uk	Alison Banwell	Scott Polar Research Institute	01-25-11	

611	dean@passcal.nmt.edu	dean	IRIS/PASSCAL	03-03-11
612	jbox.greenland@gmail.com	Jason Box	Byrd Polar Research Center	01-25-11
613	rejean.boudreau@videotron.ca	Regg	personal	03-02-11
614	emily.pilinski@colorado.edu	Emily Pilinski	University of Colorado Boulder	01-27-11
615	rye@atm.ox.ac.uk	Cameron Rye	University of Oxford	01-27-11
616	dk43@duke.edu	DOHYUK KANG	DUKE UNIVERSITY	03-03-11
617	Ole.Humlum@geo.uio.no	Ole Humlum	Department of Geosciences, University of Oslo	01-27-11
618	yuegeng2008@u.northwestern.edu	Yue Geng	Northwestern University	02-01-11
619	dan.johnson@uleth.ca	Dan Johnson	University of Lethbridge, Alberta, Canada	02-03-11
620	organicmobility@gmail.com	David Irwin	Pratt Institute	02-05-11
621	organicmobility@gmail.com	David Irwin	Pratt Institute	02-10-11
622	TRaach@langlauf.com	Thomas Raach	Langlauf.company	02-10-11
623	TRaach@langlauf.com	Thomas Raach	Langlauf.company	02-16-11
624	lindsey.nicholson@uibk.ac.at	Lindsey Nicholson	UNIS / University of Innsbruck	02-16-11
625	soroushr@buffalo.edu	soroush rezvanbehban	University at Buffalo	02-16-11
626	pdjakow@gmail.com	Piotr Djakow	none	02-23-11
627	afb39@cam.ac.uk	Alison Banwell	Scott Polar Research Institute	03-07-11
628	csyoannd@swansea.ac.uk	Yoann Drocourt	swansea university	02-25-11
629	csyoannd@swansea.ac.uk	Yoann Drocourt	swansea university	02-25-11
630	pdjakow@gmail.com	Piotr Djakow	none	02-26-11
631	jbox.greenland@gmail.com	Jason Box	Byrd Polar Research Center	03-01-11
632	vasilii.petrenko@colorado.edu	Vasilii Petrenko	INSTAAR	03-01-11
633	plp@dmi.dk	Philippe Lucas-Picher	Danish Meteorological Institute	03-03-11
634	john.burkhart@nilu.no	John Burkhart	University of California, Merced	03-03-11
635	stef.lhermitte@knmi.nl	Stef Lhermitte	KNMI	03-05-11
636	malin.johansson@natgeo.su.se	Malin Johansson	Stockholm University	03-05-11
637	bruce.vaughn@colorado.edu	Bruce Vaughn	INSTAAR	03-10-11
638	SWong01@gmail.com	Sandy Wong	CRREL	03-10-11
640	lilja@gfy.ku.dk	Susanne Lilja Buchardt	Centre for Ice and Climate	03-11-11
641	jjaimoe@gmail.com	Julie Miller	University of Utah / Department of Geography	03-16-11
642	k.Jeckel@web.de	Klaus Jeckel	private	03-16-11
643	tornado.f5@mail.ru	Igor	unknown	03-21-11
644	gro5002@psu.edu	Gilman	Penn State University	03-21-11
645	nolwenn.chauche@locean-ipsl.upmc.fr	Nolwenn Chauché	LOCEAN UPMC	03-23-11
646	mbprocunier@gmail.com	Matt Procunier	Nipissing University	03-25-11
647	palexander@gc.cuny.edu	Patrick Alexander	City College of New York	03-25-11
648	brandt@atmos.washington.edu	Richard Brandt	University of Washington, Dept. of Atmospheric Sciences	03-31-11
649	taohe83@gmail.com	Tao He	University of Maryland, USA	04-01-11
650	tlaepple@awi.de	Thomas Laepple	AWI Germany / Harvard University	04-01-11
651	hma@geus.dk	Horst Machguth	GEUS, Geological Survey od Greenland and Denmark, Copenhagen	04-06-11
652	vasilii.petrenko@colorado.edu	Vasilii Petrenko	INSTAAR, U Colorado	04-07-11
653	hong909@kopri.re.kr	Sangbum Hong	Korea Polar research Institute	
654	hong909@kopri.re.kr	Sangbum Hong	Korea Polar research Institute	04-13-11
655	mniwano@mri-jma.go.jp	Masashi Niwano	Meteorological Research Institute / Japan Meteorological Agency	04-20-11
656	rmj152@psu.edu	Randy Justin	Penn State University	04-20-11
657	rmj152@psu.edu	Randy Justin	Penn State University	04-20-11
659	rmj152@psu.edu	Randy Justin	Penn State University	04-27-11
660	rmj152@psu.edu	Randy Justin	Penn State University	04-27-11

661	r.j.carr@durham.ac.uk	Rachel Carr	Durham University	04-27-11
662	roman.sandner@enveo.at	Roman Sandner	ENVEO IT	04-27-11
663	duan.29@osu.edu	Jianbin Duan	the Ohio State University	05-01-11
664	ben.castellani@noaa.gov	Ben Castellani	NOAA / ESRL	05-11-11
665	stroeve@kryos.colorado.edu	Julienne Stroeve	NSIDC	05-16-11
666	emmihenna.jaaskelainen@fmi.fi	Emmihenna Jä-äskeläinen	Ilmatieteen laitos	05-23-11
667	zzzaaaplm@yahoo.com	Bob	unknown	05-23-11
668	ann-marie.berggren@geo.uu.se	Ann-Marie Berggren	Uppsala University	05-23-11
669	webmaster@mherrera.org	Maximiliano Herrera	Extreme Temperatures	06-10-11
670	cmc@live.it	Carlo Carmagnola	CNRS - France	06-10-11
672	jentoneill@gmail.com	Jennifer ONeill	NASA	06-10-11
673	webmaster@mherrera.org	Maximiliano Herrera	Extreme Temperatures	06-13-11
674	arennerm@rci.rutgers.edu	Asa Rennermalm	Rutgers, The State University of New Jersey	06-18-11
675	indrani@ldeo.columbia.edu	Indrani Das	Columbia University	06-18-11
676	indrani@ldeo.columbia.edu	Indrani Das	Columbia University	06-18-11
677	indrani@ldeo.columbia.edu	Indrani Das	Columbia University	06-18-11
678	indrani@ldeo.columbia.edu	Indrani Das	Columbia University	06-18-11
679	vasilii.petrenko@colorado.edu	Vasilii Petrenko	INSTAAR, U Colorado	06-18-11

Table 2.1: User requests for GC-Net data since January 2010. Approximately 35 Giga-Bytes of data were distributed via the FTP server for a total of 248 user requests.

2.6 GC-Net Citation List

This list represents publications that made use of Greenland Climate Network (GC-Net) data.

Abdalati, W. and K. Steffen, Greenland ice sheet melt extent: 1979-1999, *J. Geophys. Res*., 106(D24), 33,983-33,989, 2001.

Allison, I., et al., The Copenhagen Diagnosis,: Updating the World on the Latest Climate Change, The University of South Wales Climate Change Research Center (CCRC), Sydney, Australia, pp.60, ISBN 978-0-9873216-0-6, 2009.

Becker, O.O. and K. Steffen, Above Zero, Hatje Cantz Verlag, Austria, pp.175, ISBN 978-3-7757-2437-1, 2009.

Box, J.E., D.H. Bromwich1, B.A. Veenhuis, Le-S. Bai, J.C. Stroeve, J.C. Rogers, K. Steffen, T. Haran, S.-H.. Wang, Greenland ice sheet surface mass balance variability (1988-2004) from calibrated Polar MM5 output, *J.Clim*., 2005.

Box, J. E., Surface Water Vapor Exchange on the Greenland Ice Sheet Derived from Automated Weather Station Data, PhD Thesis, Department of Geography, University of Colorado, Boulder, CO, Cooperative Institute for Research in Environmental Sciences, 190 pp, 2001.

Box, J.E. and K. Steffen, Sublimation on the Greenland ice sheet from automated weather station observations, *J. Geophys. Res*., 106(D24), 33,965-33,982, 2001.

Bromwhich, D., J. Cassano, T. Klein, G. Heinemann, K. Hines, K. Steffen and J. Box, Mesoscale modeling of katabatic winds over Greenland with Polar MM5, *Mon. Weather Review,* 129, 2290-2309, 2001.

Cassano, J.J., J.E. Box, D.H. Bromwich, L. Li, and K. Steffen, Evaluation of Polar MM5 simulations of Greenland's atmospheric circulation, *J. Geophys. Res*., 106(D24), 33,867-33,890, 2001.

Colgan, W., H. Rajaram, R. Anderson, K. Steffen, T. Phillips, I. Joughin, H.J. Zwally , and W. Abdalati, The annual glaciohydrology cycle in the ablation zone of the Greenland ice sheet: Part I. Hydrology Model, *J. Glaciol*., 57(204), 2011.

Cullen, N., and K. Steffen, Unstable near-surface boundary conditions in summer on top of the Greenland ice sheet., *Geophys. Res. Lett*., 28(23), 4491-4494, 2001.

Cullen, N.J., K. Steffen, and P. D Blanken, Nonstationarity of Turbulent Heat Fluxes at Summit, Greenland, *Boundary-Layer Meteorology*, DOI 10.1007/s10546-006-9112-2, 2006.

Davis, C.H. and D.M. Segura, An algorithm for time-series analysis of ice sheet surface elevations from satellite altimetry, IEEE *Transactions on Geoscience & Remote Sensing,* 39(1), 202-206, 2001.

Dassau, T.M., A. Sumer, S. Koeniger, P. Shepson, J. Yang, R. Honrath, N. Culen, K. Steffen, Investigation of the role of the snowpack on atmospheric formaldehyde chemistry at Summit, Greenland, *J. Geophys. Res*., 107(D19), ACH 9.1-14, 36, 2595-2608, 2002.

Ettema, J., M. R. van den Broeke, E. van Meijgaard, W. J. van de Berg, J. E. Box, and K. Steffen, Climate of the Greenland ice sheet using a high-resolution climate model, Part 1: Evaluation, *The Cryosphere*, 4, 511–527, doi:10.5194/tc-4-511-2010,2010.

Fausto, R.S., A.P. Ahlstram, D. Van As, S.J. Johnsen, P.L. Langen , and K.Steffen, Improving surface boundary conditions with focus on coupling snow densification and meltwater retention in large-scale ice sheet models of Greenland, *J. Glaciol*., 55(193), 869-878, 2009.

Hall, D.K., J.E. Box, K.A. Casey, S.J. Hook, C.A. Shuman and K. Steffen, Comparison of satellite-derived and in-situ observations of ice and snow surface temperatures over Greenland, *Remote Sensing of the Environment*, 112(10), 3739-3749, 2008.

Hanna , E., P. Huybrechts, K. Steffen, J. Cappelen, R. Huff, Ch. Shuman, T. Irvine-Fynn, S. Wise, and M. Griffiths. Increased runoff from melt from the Greenland Ice Sheet: a response to global warming. *J. Climate,* 21, 331-341, DOI: 10.1175/2007JCLI1964.1, 2008.

Hanna,H., P.Huybrechts, I. Janssens, J..Cappelen, K. Steffen, and A. Stephens, Runoff and mass balance of the Greenland ice sheet: 1958–2003, *J. Geophys. Res*., 110, D13108, doi:10.1029/2004JD005641, 2005.

Hanna, E. and P. Valdes, Validation of ECMWF (re)analysis surface climate data, 1979-1998, for Greenland and implications for mass balance modeling of the Ice Sheet, Intern. *J. Clim*., 21, 171-195, 2001.

Helmig, D, J. Boulter, D. David, J. Birk, N. Cullen, K. Steffen, B. Johsnon, S. Oltmans, Ozone and meteorological boundary-layer conditions at Summit, Greenland, *Atm. Environm*., 36, 2595-2608, 2002.

Herzfeld, U.C., J.E. Box, K. Steffen, H. Mayer, N. Caine, and M. Losleben, A case study on the influence of snow and ice surface roughness on melt energy, Zeitschrift für Gletscherkunde und Glazialgeology, 39, 1-42, 2006.

Honrath, R.E. Y.Y. Lu, M.C. Peterson, J.E. Dibb, M.A. Arseault, N.J. Cullen, and K. Steffen. Vertical fluxes of NOx, HONO, and HNO3 above the snowpack at Summit, Greenland. *Atm. Environm*, 36, 2629-2640, 2002.

Klein, T., G. Heinemann, D. H. Bromwich, J. J. Cassano and K. M. Hines, Mesoscale modeling of katabatic winds over Greenland and comparisons with AWS and aircraft data, *J. Met. Atmos. Phys*., 8(1/2), 115-132, 2001.

Klein, T., G. Heinemann, Simulations of the katabatic wind over the Greenland ice sheet with a 3D model for one winter month and two spring months, Report of the DAAD/NSF project 315-PP, 1999.

McGrath, D., K. Steffen, I. Overeem, S. Mernild, B. Hasholt, and M. van der Broeke, Sediment plumes as a proxy for local ice sheet runoff on the Kangerlussuaq Fjord, West Greenland. *J. Glaciol*., 56(199), 813-821, 2010.

Mernild, S.H., G. E. Liston, K. Steffen, M. van den Broeke, and B. Hasholt, Runoff and mass balance simulations from the Greenland Ice Sheet at Kangerlussuaq (Søndre Strømfjord) in a 30-year perspective, 1979–2008, *The Cryosphere*, 4, 231-242, doi:10.5194/tc-4-231-2010, 2010.

Mernild, S.H., G. E. Liston, I.M. Howat, Y. Ahn, K. Steffen, B.H. Jakobsen, B. Hasholt, B. Fog, and D. van As, Freshwater flux to Sermilik Fjord, SE Greenland, *The Cryosphere.*, 4, 453-465, 2010, doi:10.5194/tcd-4-453-2010.

Merlind, S.H., G. Liston, K. Steffen, and P. Chylek, Meltwater flux and runoff modeling in the ablation area of Jakobshavn Isbrae, West Greenland. *J. Glaciol.*, 56(195), 20-32, 2010.

Mernild, S.H., G.E. Liston, C.A. Hiemstra, K. Steffen, E. Hanna, and J.H. Christensen, Greenland Ice Sheet surface mass-balance modeling and freshwater flux for 2007, and in a 1995–2007 perspective, I, DOI: 10.1002/hyp.7354, 2009.

Mernild, S.D., G.E. Liston, C.A., Hiemstra, C.A., and K. Steffen, Record 2007 Greenland ice sheet surface melt extent and runoff, *EOS*, 90, 13-14, (Jan 13), 2009.

Mernild, S., G. Liston, Ch. Hiemstra, K. Steffen, E. Hanna, and J.H. Christensen, Greenland Ice Sheet surface mass-balance modeling and freshwater flux for 2007, and in a 1995–2007 perspective. *J. Hydrometeorology*, 9, DOI: 10.1175/2008JHM957.1, 2008.

Mernild, S., G. Liston, Ch. Hiemstra, K. Steffen, Surface melt area and water balance modeling on the Greenland ice sheet 1995-2005, *J. Hydrometeorology*, 9, DOI: 10.1175/2008JHM957.1, 2008.

Mosley-Thompson, E., J.R. McConnell, R.C. Bales, Z. Li, P.-N. Lin, K. Steffen, L.G. Thompson, R. Edwards, D. Bathke, Local to regional-scale variability of annual net accumulation on the Greenland ice sheet from PARCA cores, *J. Geophys. Res*., 106 (D24), 33,839-33852, 2001.

Munneke, P.K., M. R. van den Broeke, C. H. Reijmer, M. M. Helsen, W. Boot, M. Schneebeli, and K. Steffen, The role of radiation penetration in the energy budget of the snowpack at Summit, Greenland. *The Cryosphere Discuss*., 3, 277-306, 2009.

Nghiem, S.V., , K. Steffen, G. Neumann, and R. Huff, Snow Accumulation and Snowmelt Monitoring in Greenland and Antarctica, International Association of Geodesy Publication*, Dynamic Planet*, Chapter 5, 31-38, 2007.

Nghiem,S,V., K. Steffen, G. Neumann, and R. Huff, Mapping of ice layer extent and snow accumulation in the percolation zone of the Greenland ice sheet, *J. Geophys., Res*., 110, F02017, doi:10.1029/2004JF000234, 2005.

Nghiem, S.V., K. Steffen, R. Kwok, and W.Y. Tsai, Diurnal variations of melt regions on the Greenland ice sheet*, J. Glaciol*., 47(159), 539-547, 2001.

Njastad, K., R. Armstrong, R.W. Corell, D.D. Jensen, K.R. Leslie, A. Rivera, Y. Tandong, J.D. Winther, and K. Steffen. Melting snow and ice: call for action, Center for Ice, Climate and Ecosystems, Norwegian Polar Institute, pp.92, ISBN 978-82-7666-264-1, 2009.

Nolin, A. and J. Stroeve, The Changing Albedo of the Greenland Ice Sheet: Implications for Climate Change, *Ann. Glaciol.*, 25, 51-57, 1997.

Orr, A., E. Hanna, J. Hunt, J. Cappelen, K. Steffen and A. Stephens, Characteristics of stable flow over southern Greenland, *Pure and Applied Geophysics* (PAGEOPH), 161(7), 2004.

Painter, T.H., N.P. Molotch, M. Cassidy, M. Flanner, and K. Steffen, Contact spectroscopy for determination of stratigraphy of snow grain size, *J. Glaciol*, 53(180) 121-127, 2007.

Parry, V., P. Mair, J. Scott, B. Hubbard, K. Steffen, and D. Wingham, Investigations of meltwater refreezing and density variations in the snowpack and firn within the percolation zone of the Greenland Ice Sheet, *Ann. Glaciol*., 46, 621-68, 2007.

Phillips, T., S. Leyk, H. Rajaram, W. Colgan, W. Abdalati, and K. Steffen, Modeling moulin distribution on Sermeq Avannarleq Glacier using ASTER and WorldView imagery and fuzzy set theory, *Remote Sensing of the Environment*, 115, 2292-21301, 2011.

Phillips, T., H. Rajaram, K. Steffen, Cryo-hydrologic warming: A potential mechanism for rapid thermal response of ice sheets, *Geophys. Res. Lett*., 37, L20503, doi:10.1029/2010GL044397, 2010.

Rial., J., C. Tang, and K. Steffen, Glacial Rumblings from Greenland's Jakobshavn Ice Stream, *J. Glaciol.*, 15(191) 398-399, 2009.

Serreze, M., J. Key, J. Box, J. Maslanik, and K. Steffen, A new monthly climatology of global radiation for the Arctic and comparison with NCEP-NCAR reanalysis and ISCCP-C2 field, *J. Climate*, 11, 121-136, 1998.

Shuman, C., K. Steffen, J. Box, and C. Stearn, A dozen years of temperature observations at the Summit: Central Greenland automatic weather stations 1987-1999, *J. Appl. Meteorol*., 40(4),741-752, 2001.

Smith, L.C., Y. Sheng, R.R. Foster, K. Steffen, K.E. Frey, and D.E. Alsdorf, Melting of small Arctic ice caps observed from ERS scatterometer time series, *Geophys. Res. Lett.,* 30(20), CRY 2-14, 2003.

Steffen, K., S.V. Nghiem, R. Huff, and G. Neumann, The melt anomaly of 2002 on the Greenland Ice Sheet from active and passive microwave satellite observations, *Geophys. Res. Lett*., 31(20), L2040210.1029/2004GL020444, 2004.

Steffen, K., and J.E. Box, Surface climatology of the Greenland ice sheet: Greenland climate network 1995-1999*, J. Geophys. Res*., 106(D24), 33,951-33,964, 2001.

Steffen, K., W. Abdalati, and I. Serjal, Hoar development on the Greenland ice sheet, *J. Glaciol*., 45(148), 63-68, 1999.

Steffen, K., J. E. Box and W. Abdalati, Greenland climate network: GC-Net, CRREL, 98-103 pp., 1996.

Steen-Larsen, H.C., V. Masson-Delmotte, J. Sjolte, S.J. Johnsen, B.M. Vinther, F-M Bréon, H.B. Clausen, D. Dahl-Jensen, S. Falourd, X. Fettweis, H. Gallée , J. Jouzel, M. Kageyama, H. Lerche, B. Minster, G. Picard, H. J. Punge, C. Risi, D. Salas, J. Schwander, K. Steffen, A E. Sveinbjörnsdóttir, A. Svensso , J. White, Understanding the climatic signal in the water stable isotope records from the NEEM shallow firn/ice cores in North-West Greenland, *J. Geophys. Res.,* 116 , 2011.

Stroeve, J., Assessment of Greenland Albedo Variability from the AVHRR Polar Pathfinder Data Set, *J. Geophys. Res*., 106(D24), 33,989-34,006, 2001.

Stroeve, J., and A. Nolin, 1997. The changing albedo of the Greenland ice sheet: implications for climate modeling, *Ann. of Glaciol*., 25, 51-57.

Stroeve, J, J. E. Box, J. Maslanik, J. Key, C. Fowler, Intercomparison between in situ and AVHRR Polar Pathfinder-derived surface albedo over Greenland, *Remote Sensing of the Environment*, 75(3), 360-374, 2001.

Thomas, R., and PARCA instigators, Program for Arctic Regional Climate Assessment (PARCA): Goals, key findings, and future directions*, J. Geophys. Res*., 106(D24), 33,691-33706, 2001.

Thomas, R.H., W. Abdalati, E. Frederick, W.B. Krabill, S. Manizade, and K. Steffen, Investigation of surface melting and dynamic thinning on Jakobshavn Isbrea, Greenland, J. Glaciol., 49(165), 231-239, 2003.

Wang, L., M. Sharp, B. Rivard, and K. Steffen, Melt duration and ice layer formation on the Greenland ice sheet, 2000-2004, *J. Geophys. Res*., 112, F04013, doi:10.1029/2007JF000760 2007.

Zwally, H.J. W. Abdalati, T. Herring, K. Larsen, J. Saba, and K. Steffen. Surface melt-induced acceleration of Greenland ice-sheet flow, *Science*, 297, 218-222, 2002.

3. Results

3.1 Swiss Camp Climatology: 1991-2010

3.1.1 Temperature

The mean annual air temperature at Swiss Camp is -12.0° C (1991-2010), with the coldest monthly temperature in February (-32° C) and the warmest monthly temperature in July (1.8 C in 2010) (Fig. 3.1.1). Summer months with above freezing occurred in 1995, and from 1997– present.

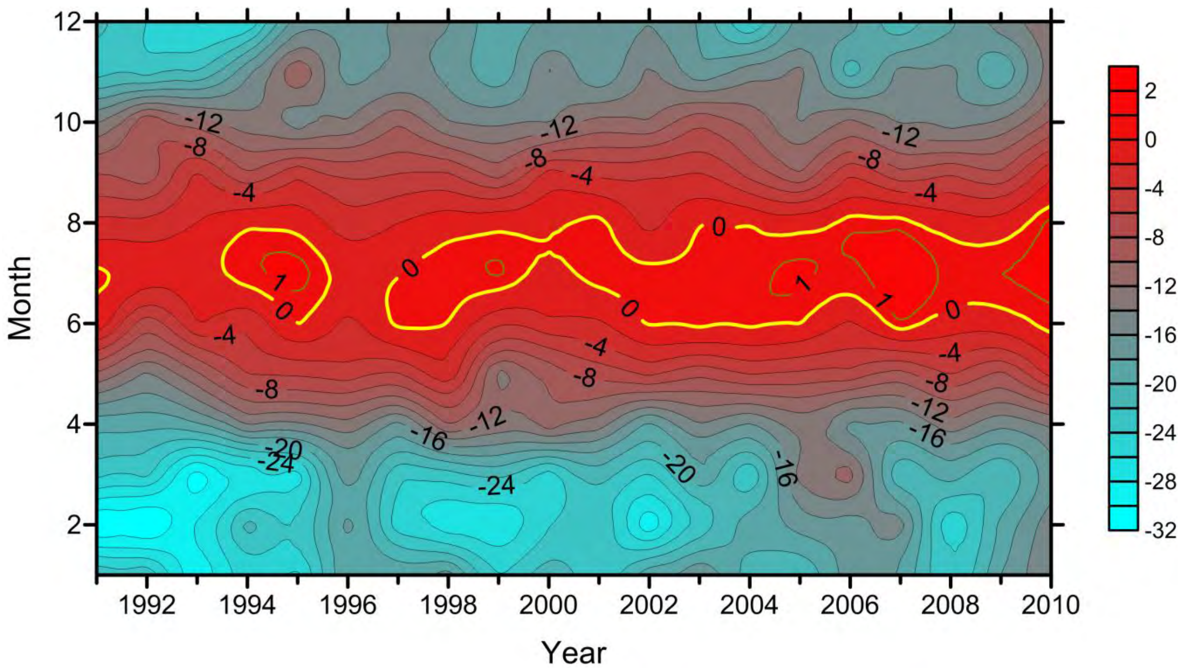

Figure 3.1.1: Interannual variability of monthly mean air temperatures (1991 – 2010) at the Swiss Camp, located at the equilibrium line altitude on the western slope of the Greenland ice sheet.

The mean annual temperature has increased by 4.2 ºC between 1991 and 2010 (2.2 ºC per decade) using a linear regression model as shown in Figure 3.1.2. The minimum temperature in 1992 was the result of the aerosol loading caused by the Mt. Pinatubo eruption. The linear regressing model at 95% confidence shows that the Pinatubo cooling and also the subsequent warming from the mid 90's were outside the 95% level of confidence. The warming that occurred since 2000 to present shows approximately the same trend then the 19-year time series. The warmest mean annual temperature was recorded with -8.0º C in 2010.

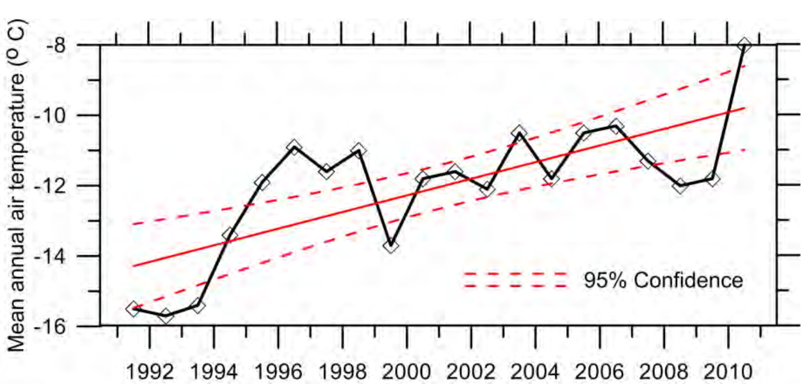

Figure 3.1.2: Swiss Camp mean annual temperature 1991 – 2010 (black line) with a linear regression model (red line) and 95% confidence levels (dashed red lines).

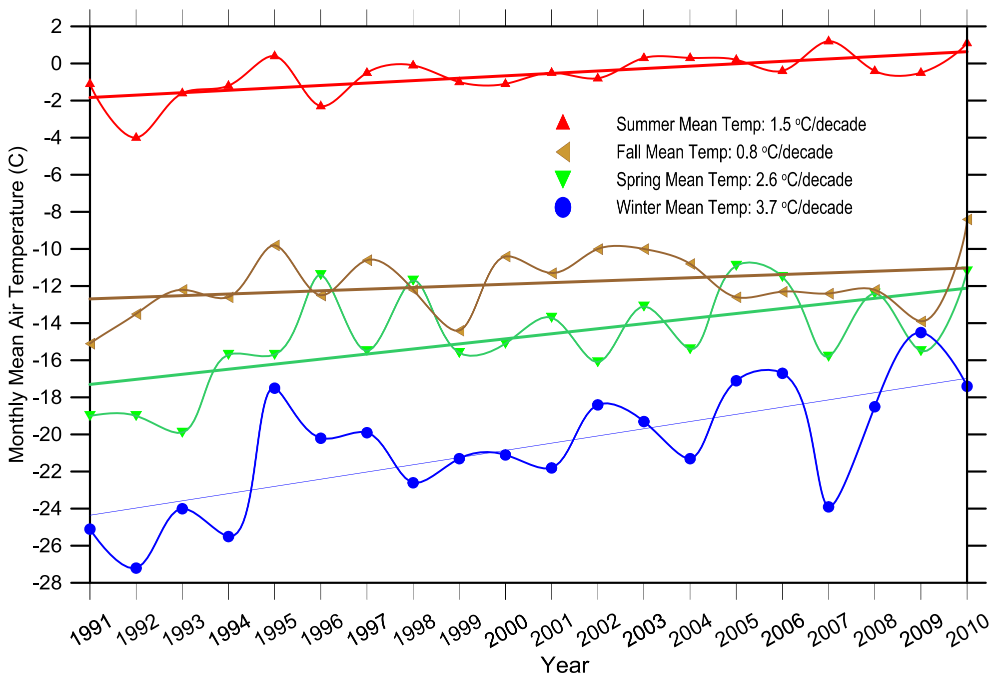

Figure 3.1.3: Swiss Camp mean seasonal temperatures for summer (JJA), spring(MAM), fall (SON), and winte (DJF)r for 1991 – 2009

The statistical analysis of the Swiss Camp air temperature record reveals large interannual variability in all seasons with increasing temperatures throughout the recording period (Fig. 3.1.3). The mean spring temperature increased from -17.5º C to -12.0º C, and fall temperature increased from -12.6º C to -11.0º C between 1991 and 2010, using a linear model. The winter temperature showed the largest increase of 7º C, whereas summer temperatures increased 3.0º C during the 19 years (1991 – 2010). The climate record at Swiss Camp shows a clear warming trend that started around 1995.

3.1.2 Radiation

Radiation has been monitored continuously at Swiss Camp since 1993. The time series of mean monthly net radiation values is shown in Figure 3.1.4 (1993 – 2010). The largest monthly mean net radiation was found in the summer 1995 and 2007 (65 W m^{-2}), coincident with air temperatures above freezing, indicating a strong albedo-feedback mechanism at the ELA. Net radiation in 2010, the warmest year and summer month on record was 50 W $m^{-2.}$ Most of the annual snow cover melted and the bare ice surface was exposed, reducing the monthly albedo value to 0.4 (Fig.3.1.5).

It is worth discussing the three anomalous periods 1995, 1998, and 2001-2010 (Fig. 3.1.4). The summer season is characterized by a positive net radiation flux, which is indicative of the length of the melting season. High net radiation values can either be the result of low albedo values (i.e., 2003-2010, Fig. 3.1.5), reduced cloudiness (increase in insolation), or increase in atmospheric temperatures (increase in long-wave radiation). The mean summer net radiation has been higher during the new millennium (30 W m^{-2}) compared to the previous decade, with the exception of record high values in 1995, as a result of increased atmospheric temperatures leading to increase in surface melt (albedo reduction).

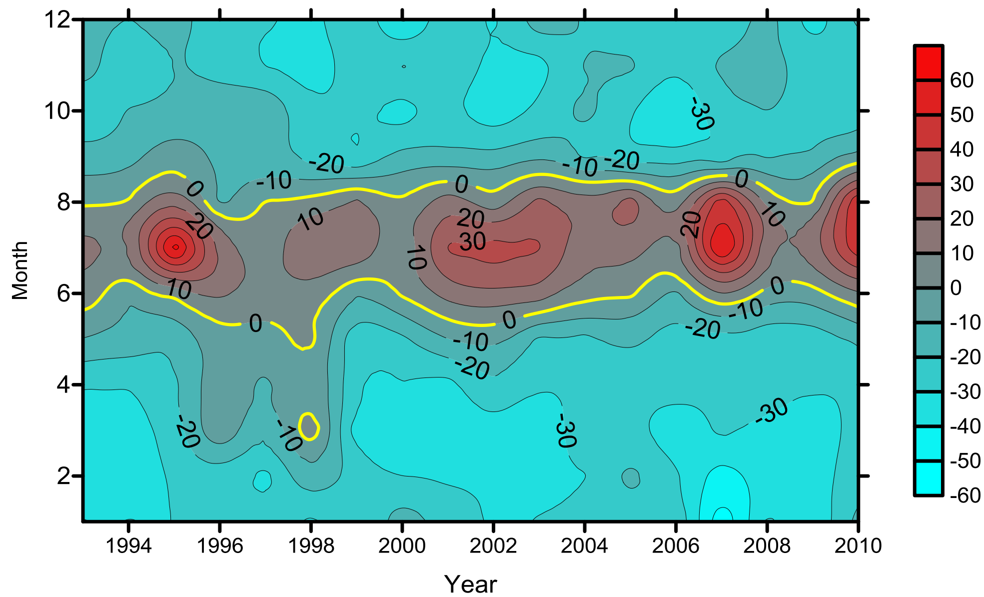

Figure 3.1.4: Interannual variability of monthly net radiation at the Swiss Camp (1993-2010).

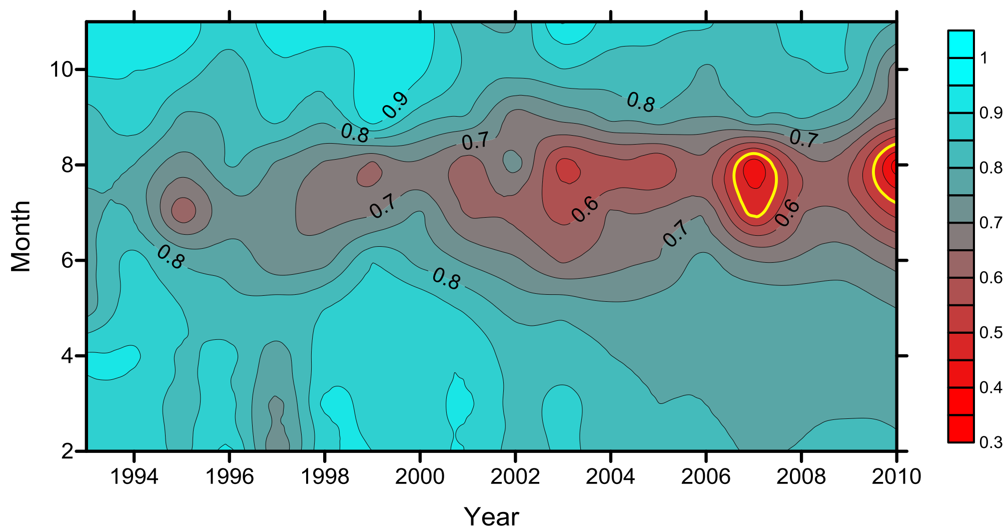

Figure 3.1.5: Interannual variability of monthly mean albedo at the Swiss Camp (1993 – 2010). Albedo at 0.5 is shown with a yellow contour line. The lowest surface albedo with 0.35 was recorded in summer 2010.

3.1.3 Accumulation and ablation

Interannual variability of snow accumulation varies between 0.07 and 0.70 m water equivalent (w.e.), whereas the snow and ice ablation varies between +0.35 (net gain) and -1.8 m (net loss) (w.e.) for the time period 1990-2010. The mean net surface mass balance hovered around zero in the 90's with small deviations from (zero (no mass change) (Fig. 3.1.6), whereas a net mass loss is apparent starting in 2002 to present. The equilibrium line altitude (ELA) is no longer located at Swiss Camp (1100 m elevation) with a net surface lowering of 5.5 m, and moved tent's of kilometers inland.

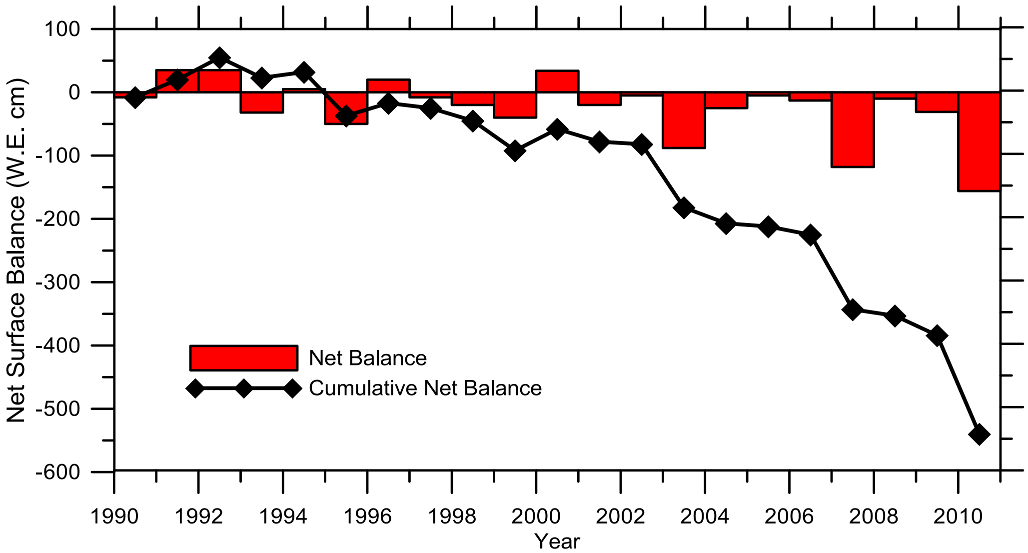

Figure 3.1.6: Net surface mass balance for the Swiss Camp location (red bars), and cumulative net balance (thick black line) for Swiss Camp 1990 – 2010.

3.2 Moulin and Englacial Modelling

3.2.1 Modeling effort background

At present, Greenland's mass loss appears to be equally split between surface mass balance (i.e. melt and runoff) and ice dynamics (i.e. ice discharge; *van den Broeke et al.*, 2009). Predicting the relative contributions of these two terms to future sea level rise is complicated by potential non-linear feedbacks. Generally, however, the future ice dynamic contribution is regarded as more difficult to forecast than its surface mass balance counterpart. This is due to the inability to establish the mechanism responsible for the recent widespread acceleration of outlet glaciers (*Rignot and Kanagaratnam*, 2006; *Joughin et al*., 2010). Over the past decade at least five distinct mechanisms have been proposed to explain the recent acceleration of Greenland outlet glaciers: (i) observations suggest that increased surface meltwater production can results in enhanced basal sliding velocity on a variety of time-scales (*Zwally et al*., 2002; *Shepherd et al.*, 2009; *Bartholomew et al.*, 2010); (ii) the recent acceleration of major glaciers may be a short-term dynamic re-adjustment to a perturbation of surface ablation (*Thomas*, 2004); (iii) the recent acceleration may be the onset of a long-term response to increased effective driving stress stemming from a loss of terminus back-stress (*Howat et al*., 2008; *Joughin et al*., 2008); (iv) glacier acceleration can result from decreased effective basal pressure (ice pressure minus water pressure) due to surface ablation-induced thinning of outlet glaciers with no corresponding change in subglacial water pressure (*Pfeffer*, 2007); and finally (v), as ice sheets appear to be susceptible to relatively rapid changes in ice temperature via cryo-hydrologic warming (*Phillips et al*., 2010), the warming of ice in lateral shear zones can result in an increase in ice velocities and discharge (*van der Veen et al*., in press).

A portion of the research conducted over the past year under the auspices of this grant has focused on better understanding mechanisms (i) and (iii). We have developed models to describe both the hydrology and ice flow of the Sermeq (Glacier) Avannarleq flowline. Sermeq Avannarleq, a tidewater glacier that calves into a sidearm of Jakobshavn Fiord, is located downstream from CU/ETH ("Swiss") Camp. The Sermeq Avannarleq flowline runs 530 km upglacier from the tidewater terminus of Sermeq Avannarleq (km 0), through JAR2 automatic weather station (km 14), within 2 km of Swiss Camp (km 46), to the main ice divide of the Greenland Ice Sheet (km 530 at

71.54 °N, 37.81 °W; Figure 3.2.1). The Sermeq Avannarleq ablation zone appears to experience an annual velocity cycle that is "typical" of the western margin of the Greenland Ice Sheet (*Joughin and others*, 2008). This annual velocity cycle, which is evident in GPS observations at Swiss Camp and InSAR observations at JAR2, is comprised of a summer speedup event followed by a fall slowdown event (Figure 3.2.2). At this onset of this project, it was not evident whether seasonally enhanced basal sliding (mechanism (i)) or seasonally reduced terminus back-stress (mechanism (iii)) was responsible for this annual velocity cycle. Our findings now suggest that enhanced basal sliding is more important than reduced terminus back-stress in determining inland ice velocities.

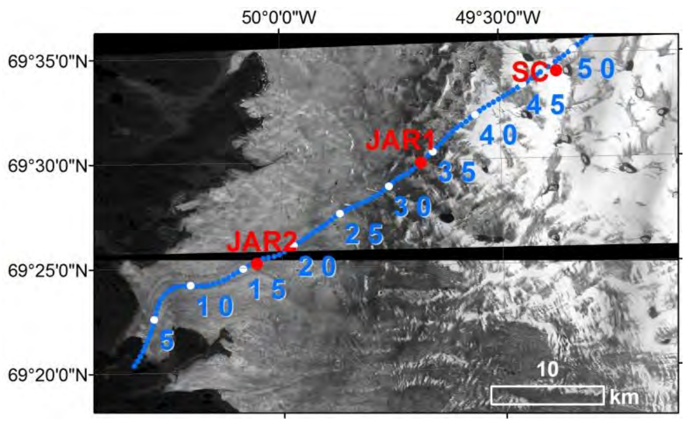

Figure 3.2.1: The terminal 55 km of the Sermeq Avannarleq flowline overlaid on a panchromatic WorldView-1 image (acquired 15 July 2009) with distance from the terminus indicated (km). GC-Net weather station locations are denoted in red.

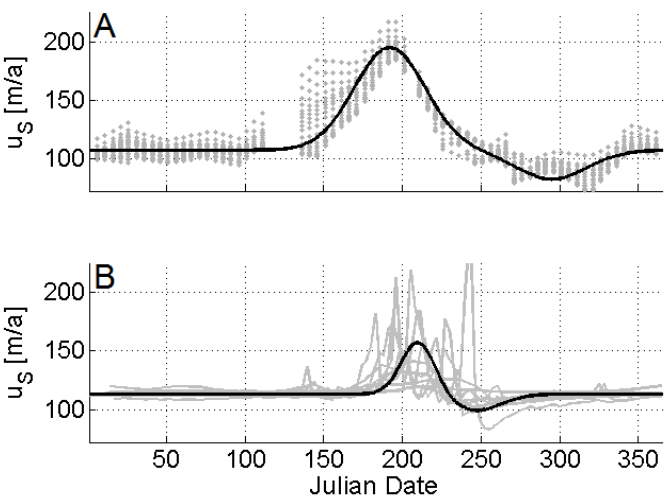

Figure 3.2.2: A: Observed InSAR ice surface velocities over the 2005 to 2006 period at JAR2. B: GPS ice surface velocities over the 1996 to 2008 period at Swiss Camp. Black lines denote a bi-Gaussian characterization at each station.

3.2.2 Hydrology model: Basal sliding

Studies of alpine glaciers suggest that changes in basal sliding velocity are due to a combination of changes in the rate of glacier water storage (i.e. total glacier water input minus output; *Anderson et al.*, 2004; *Bartholomaus et al.,* 2008) and changes in flotation fraction (the ratio of subglacial water pressure to basal ice pressure; *Iken et al.*, 1983; *Kamb et al.*, 1994). This explains why "bursts" of basal motion are associated with meltwater "pulses", while sustained meltwater input, which eventually leads to the establishment of efficient subglacial conduits and a negative rate of change of glacier water storage, does not lead to sustained basal sliding. Changes in the rate of glacier water storage (or englacial head elevation; $\partial h_e/\partial t$) are due to changes in both the rate of meltwater production (i.e. glacier "input") and the rate of water loss from a glacier, governed by the efficiency of subglacial transmissivity via cavities and conduits (i.e. glacier "output"). We developed a hydrology model to examine the annual velocity cycle of the Sermeq Avannarleq flowline in the context of the annual hydrologic cycle.

In this conceptual model the subglacial hydraulic head is equivalent to the local englacial water table elevation (h_e). Conduits, which operate at the ice-bed interface, whose geometry evolves through time, control the horizontal water discharge (Q) within the glacier hydrologic system. Thus, h_e varies in time and space due to variable conduit inflow and outflow as well as dynamic changes in conduit storage. By enforcing water conservation, the rate of change in hydraulic head (or englacial water table elevation) at a given node along the flowline may be calculated from four terms: (i) external meltwater input I (via both surface and basal ablation per unit area) multiplied by the flow band cross width (w), (ii) internal meltwater generation due to viscous melt within the conduits (m/ρ_w), (iii) horizontal divergence of conduit discharge ($\partial Q/\partial x$), and (iv) changes in conduit storage volume (per unit length along the flowline) through time ($\partial S_c/\partial t$):

$$\varphi w \frac{\partial h_e}{\partial t} = Iw + \frac{m}{\rho_w} - \frac{\partial Q}{\partial x} - \frac{\partial S_c}{\partial t} \qquad \text{Eq. 3.2.1}$$

where φ is the bulk ice porosity at a given node and w is a cross-flow width.

Within a plausible parameter space, the model achieves a quasi-steady-state annual glacier hydrologic cycle in which hydraulic head oscillates close to flotation throughout the ablation zone (Figure 3.2.3). Flotation is briefly achieved during the summer melt season along a ~ 17 km stretch of the flowline within the ablation zone. Beneath the majority of the flowline, subglacial conduit storage "closes" (i.e. obtains minimum radius) during the winter and "opens" (i.e. obtains maximum radius) during the summer. Along certain stretches of the flowline, however, the model predicts that subglacial conduit storage remains open throughout the year. A calculated mean glacier water residence time of ~ 2.2 years implies that significant amounts of water are stored in the glacier throughout the year. We interpret this residence time as being indicative of the time-scale over which the glacier hydrologic system is capable of adjusting to external surface meltwater forcings. From comparison with surface ice velocity observations, we suggest that maximum annual ice velocities generally correspond to conditions of increasing hydraulic head during inefficient subglacial drainage in early summer. Conversely, minimum annual ice velocities generally correspond to conditions of decreasing hydraulic head during efficient subglacial drainage in early fall. Thus, the character of the annual velocity cycle is consistent to enhanced basal sliding due to increased rates of glacier water storage.

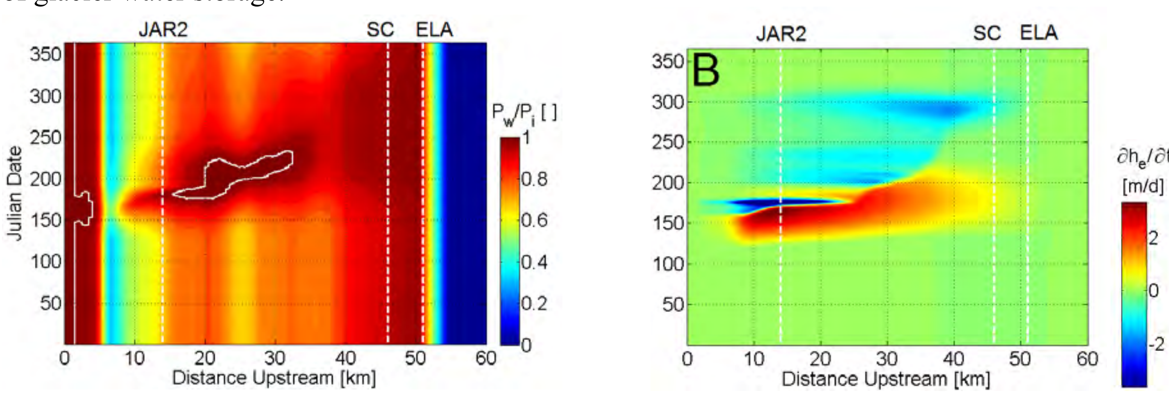

Figure 3.2.3: ***Left****: Modeled time-space distribution of flotation fraction (P_w/P_i). The white contour line denotes a flotation fraction of 1*. ***Right:*** *Modeled time-space distribution of the rate of change of hydraulic head (or englacial water table elevation; $\partial h_e/\partial t$). Colorbar saturates below -3.6 m/d. Vertical dashed lines denote the locations of JAR2, Swiss Camp and the equilibrium line.*

3.2.3 Ice flow model: Longitudinal coupling

It is also possible that the annual velocity cycle observed at Swiss Camp is due to the upstream propagation (via longitudinal coupling) of a downstream velocity signal (i.e. lower elevation enhanced basal sliding or the annual tidewater calving cycle). A previous study has suggested that 10 to 20 % of the seasonal velocity variations at Swiss Camp could be attributed to a roughly 100 % seasonal velocity increase initiated ~ 12 km downstream from Swiss Camp that is propagated upstream through longitudinal coupling (*Price et al.*, 2008). To evaluate this possibility, we introduce a depth-averaged longitudinal coupling stress (τ'_{xx}) as a perturbation to the driving stress from the shallow ice approximation in our ice flow model of the Sermeq Avannarleq (*van der Veen*, 1987; *Marshall et al.*, 2005):

$$\tau = -\rho_i g H \frac{\partial z_s}{\partial x} + 2\frac{\partial}{\partial x} \qquad \text{Eq. 3.2.2}$$

where τ is the longitudinally coupled basal driving stress, ρ_i is the density of ice, g is gravitational acceleration, H is ice thickness and z_s is ice surface slope. (9.81 m/s^2). Depth-averaged longitudinal coupling stress is calculated following the approach outlined by *van der Veen* (1987). This formulation derives longitudinal coupling stress by solving a cubic equation describing equilibrium forces independently at each node, based on ice geometry and prescribed basal sliding velocity (u_b):

$$0 = {\tau'_{xx}}^3 \;\; 2\frac{\partial z_s}{\partial x} \;\; \frac{\partial H}{\partial x} - \frac{\partial z_s}{\partial x} \;\; + H\frac{\partial^2 z_s}{\partial x^2} - \frac{1}{2} \;\; + {\tau'_{xx}}^2 \;\; \tau \;\; \frac{2}{3}\frac{\partial H}{\partial x} - \frac{3}{2}\frac{\partial z_s}{\partial x} \;\; + \qquad \text{Eq. 3.2.3}$$

$$\tau'_{xx} \;\; \tau^2 \;\; 3\frac{\partial z_s}{\partial x}\frac{\partial H}{\partial x} + \frac{3}{2}H\frac{\partial^2 z_s}{\partial x^2} - 2 \;\; \frac{\partial z_s}{\partial x}^{\;2} \;\; - \frac{1}{6} \;\; + \tau^3 \;\; \frac{2}{5}\frac{\partial H}{\partial x} - \frac{1}{4}\frac{\partial z_s}{\partial x} \;\; + \frac{1}{2A}\frac{\partial u_b}{\partial x}$$

where A is the temperature-dependent flow law parameter and u_b is basal sliding velocity.

The ice flow model suggests that it is unlikely for longitudinal coupling to explain the annual ice velocity cycle observed at Swiss Camp. Absolute longitudinal coupling stress ($|\tau'_{xx}|$) is only "significant" (defined here as > 10 % of total driving stress) along the terminal ~ 5 km of the flowline (i.e. the floating tongue; Figure 3.2.4). Upstream of an ice fall at ~ 6 km, where observed ice thickness decreases to < 300 m, the absolute longitudinal coupling stresses seldom exceed 10 % of total driving stress. Additionally, in 3D, any perturbation to the tidewater tongue would also experience rapid radial diffusion (in the *xy* plane) with distance inland. This pattern of minimal inland coupling stresses fits the theoretical observation that coupling stresses are typically only important in the terminal few kilometers of ice sheet flowlines (where surface slope increases) and where the amplitude of bed topography approaches the ice thickness (*van der Veen*, 1987).

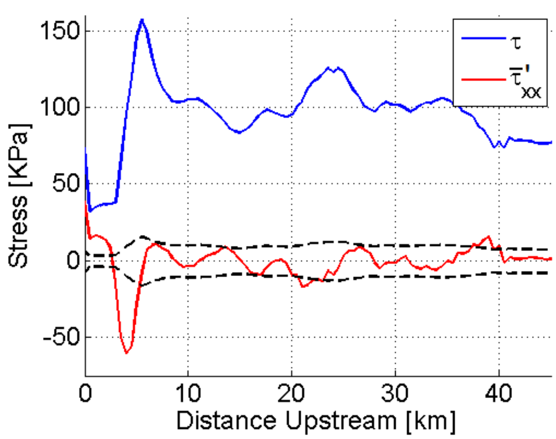

Figure 3.2.4: Total basal driving stress (τ) and longitudinal coupling stress (τ'_{xx}) along the terminal 45 km of the flowline. Dashed lines represent ± 10 % of total driving stress

Where longitudinal coupling stresses are insignificant along the Sermeq Avannarleq flowline, the forces governing ice flow can be assumed to be local in nature. Thus, at Swiss Camp, where absolute longitudinal coupling stress is < 5 % of total driving stress, the annual ice velocity cycle is more likely to be due to local glaciohydrology (i.e. local meltwater production enhancing local basal sliding) than a downstream velocity signal introduced by coupling (i.e. downstream basal sliding or terminus back-stress). This notion is supported by recent observations of a persistent englacial hydrology system in the vicinity of Swiss Camp (*Catania and Neumann*, 2009). Although the present ice geometry renders longitudinal coupling relatively unimportant inland of km 6, this does not imply that the irreversible retreat that has been observed following perturbations to the calving front of other Greenland tidewater glaciers could not potentially affect this flowline (*Nick et al.*, 2009). Other mechanisms are capable of propagating rapid wastage upstream without strong longitudinal coupling stresses, such as "irreversible tidewater retreat" that propagates upstream based on knick-point migration (*Pfeffer*, 2007).

3.2.4 Future outlook

While we have quantitatively assessed the influence of acceleration mechanisms (i) and (iii) for the Sermeq Avannarleq flowline, and established that enhanced basal sliding is likely more important than reduced terminus back-stress in determining inland ice velocities at Swiss Camp, recent observations suggest that mechanism (v), cryo-hydrologic warming, may become increasingly important. A comparison of high-resolution 1985 aerial photography with 2009 WorldView-1 imagery suggests that the area of the Sermeq Avannarleq ablation zone occupied by crevasses > 2 m wide significantly increased (13 ± 4 %) over the 24-year period (Figure 3.2.5). This expansion of existing crevasse fields, which has been readily apparent during field operations over the last decade, has been accompanied by widespread changes in crevasse orientation (up to 45 °; Figure 3.2.6). We believe the recent acceleration of Jakobshavn Isbrae (*Joughin et al*., 2008) has contributed to increased crevasse extent by altering ice flow directions, and hence reorganizing the regional ice stress field. Additionally, as the lithostatic stress opposing crevasse propagation is proportional to ice thickness, recent ice thinning in the Sermeq Avannarleq ablation zone (*Motyka et al.*, 2010) can be expected to increase crevasse propagation rate (*van der Veen*, 1998).

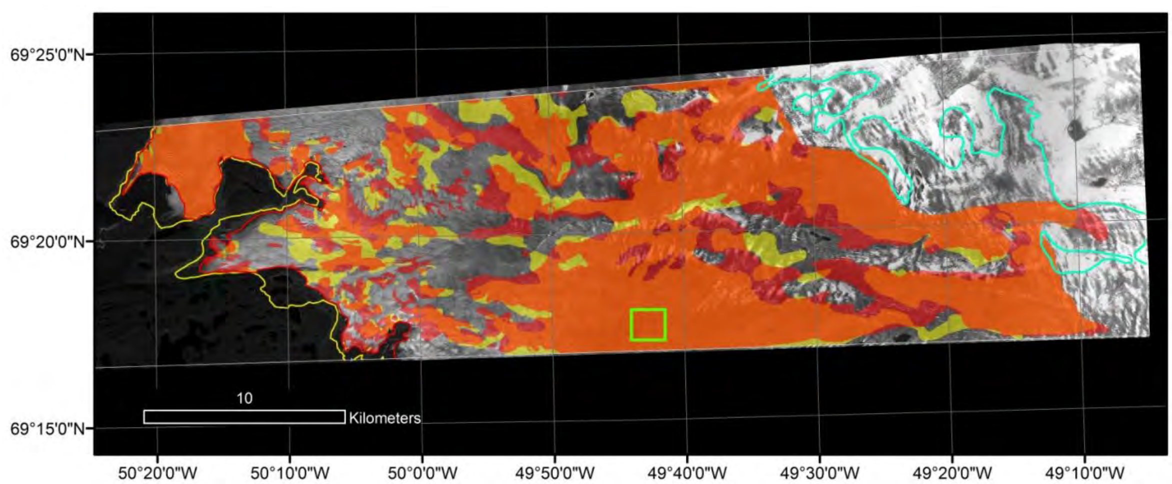

Figure 3.2.5: Crevassed areas (width > 2 m) overlaid on a panchromatic 15 July 2009 WorldView-1 image. Features in 2009 and 1985 are denoted in red and yellow, respectively, with overlapping areas in orange. The 1985 snowline (Thomsen et al., 1988) is denoted in cyan.

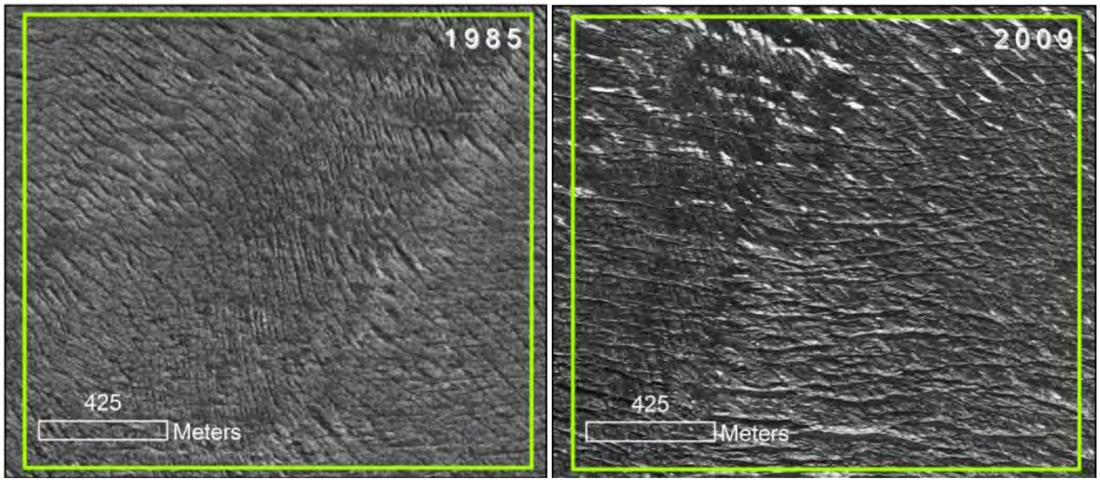

Figure 3.2.6: Crevasse orientation in a sub-region of the Sermeq Avannarleq ablation zone in 1985 and 2009.

The implications of a net transition of ice sheet area from moulin-type to crevasse-type supraglacial drainage are not completely clear. A first-order approximation suggests that the englacial transfer time of meltwater is 1-2 orders of magnitude greater (slower) in crevasse-type drainage systems than moulin-type drainage systems. As enhanced basal sliding requires meltwater to overwhelm the transmission capacity of the subglacial system, it is therefore reasonable to expect efficient moulin-type drainage (i.e. meltwater "pulses") to enhance basal sliding more than inefficient crevasse-type drainage (i.e. sustained meltwater input). Thus, an increase in crevasse area may result in a net decrease in ice sheet mass loss. Conversely, however, cyro-hydrologic warming is highly sensitive to the mean spacing of englacial hydrologic pathways (*Phillips et al.*, 2010). A net increase in crevasse extent can therefore be expected to expose an increased area of the ice sheet to closely-spaced hydrologic pathways that facilitate cryo-hydrologic warming. These pathways would be capable of warming ice temperatures and enhancing deformational ice velocities in newly crevassed regions of the ice sheet (c.f. *van der Veen et al*., in press). Thus, assessing the relative importance of mechanisms (i) and (v) is a pressing question to address with models and observations.

3.3 Glaciohydrology

Automatic Weather Station (AWS) data was used in three studies on the West Greenland ice sheet in order to get a better understanding on the processes involved in the melt of the marginal regions of the ice sheet. For these studies we used the AWS stations Crawford Point, Swiss Camp, JAR 1-3 as well as the newly added Moulin AWS station. Much of the data collected at the moulin was used in order to simulate the processes and the effects on the ablation zone. The three studies presented here involve the involved a model introducing the cryo-hydrologic system (CHS), which describes the energy transfer between melt water percolating through the ice as well as the surrounding ice. The second study used fuzzy set theory in order to locate the possible locations of moulin development. The third study, which is currently being submitted to Nature Geoscience, is a flowline model that simulates the englacial ice temperature and uses the surface velocity in order to verify its accuracy.

3.3.1 Cryo-hydrologic warming

Phillips, T., H. Rajaram, and K. Steffen (2010), Cryo-hydrologic warming: A potential mechanism for rapid thermal response of ice sheets, *Geophys. Res. Lett.,* 37, L20503, doi:10.1029/2010GL044397)

Cryo-Hydrologic (CH) warming is proposed as a potential mechanism for rapid thermal response of glaciers and ice sheets to climate warming. We present a simple parameterization to incorporate CH warming in thermal models of ice sheets using a dual-continuum concept, which treats ice and the cryo-hydrologic system (CHS) as overlapping continua with heat exchange between them. The presence of liquid water in the CHS due to surface melt leads to warming of the ice. The magnitude and timescale of CH warming is controlled by the average spacing between elements of the CHS, which is often of the order of just 10's of meters. The corresponding time-scale of thermal response is of the order of years-decades (Figure 3.3.1), in contrast to conventional estimates of thermal response time-scales based on vertical conduction through ice, which are of the order of centuries to millennia. We show that CH warming is already occurring along the west coast of Greenland (Figure 3.3.2). Increased temperatures resulting from CH warming will reduce ice viscosity and thus contribute to faster ice flow.

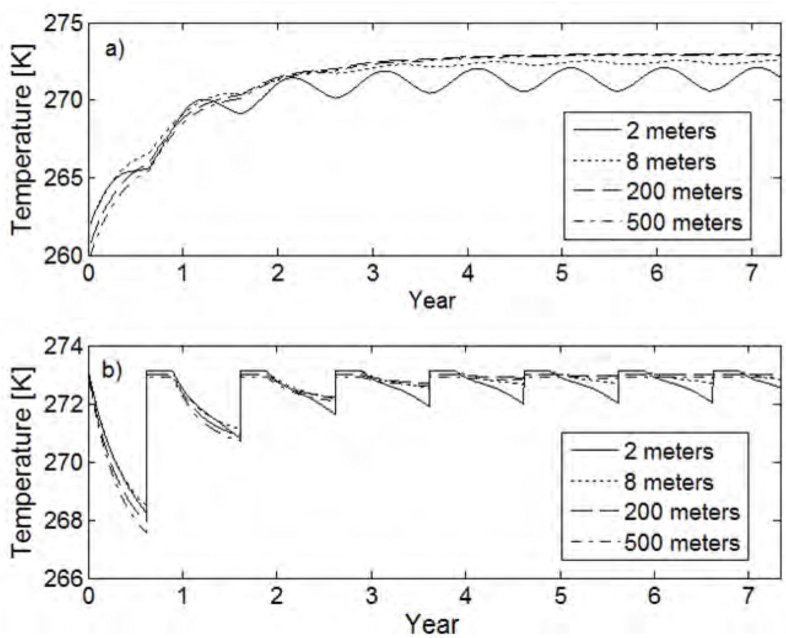

Figure 3.3.1: Evolution of temperatures in the (a) ice and (b) cryo-hydrologic columns following initiation of cryo-hydrologic activity. After a few years, the ice temperatures at 2 m and 8 m depth exhibit seasonality, but temperatures at 200 m and 500 m depth reach a new steady state.

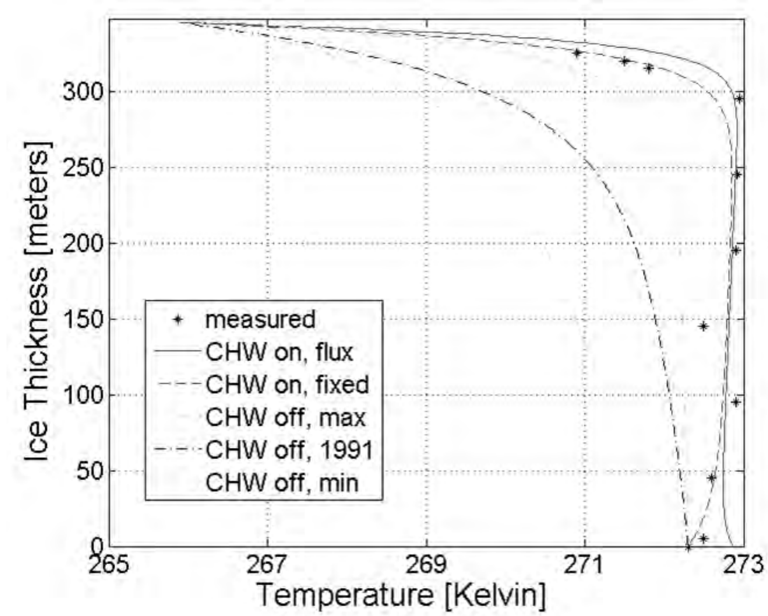

*Figure 3.3.2: Measured (symbols) and simulated (lines) temperatures for borehole TD3 on Sermeq Avannarleq, outlet glacier northeast of Ilulissat, Greenland. The two simulations with cryo-hydrologic warming (CHW on) used a specified temperature gradient of 0.0227 K/m ("gradient") and a fixed temperature equal to the measured temperature ("fixed") at the bed. Without cryo-hydrologic warming (CHW off), the base-case simulation (1991) used a fixed temperature equal to the measured temperature at the bed, the "min" and "max" curves were obtained by multiplying the u(z)*a*l term by factors of about 2 and 1/4.*

3.3.2 Fuzzy set model to locate moulin development

Phillips, T., , S. Leyk, H. Rajaram, W. Colgan, W. Abdalati, D. McGrath and K. Steffen, Modeling moulin distribution on Sermeq Avannarleq glacier using ASTER and WorldView imagery and fuzzy set theory, *Remote Sensing of Environment*, 115 (2011) 2292–2301).

A fuzzy set overlay model is used to analyze the distribution of moulins (vertical melt water conduits) on Sermeq Avannarleq ("Dead Glacier") in West Greenland in 1985 and 2008–09. Input data is derived from a historical topographic map based on airborne visible imagery and more recent WorldView-1 panchromatic imagery, as well as an Advanced Spaceborne Thermal Emission and Reflection Radiometer (ASTER) digital elevation model (DEM). GC-Net AWS data is used in order to calculate the surface mass balance and the average length of a melt season. A non-parametric best-fit model approach using a Monte Carlo simulation is used to derive the membership functions for moulin location based on three independent variables – elevation, slope and aspect – and to test for the robustness of the model (Figure 3.3.3). We determine that there is a topographic setting independent of time that favors the development of moulins in this region. Using the membership functions, and an optimal alpha cut derived for 1985, we could correctly predict the locations of ~88% of the moulins in 2008–09. In Figure 3.3.4 we can show how well our model fits the known locations of moulins. The model accounts for increased surface melt in 2008–09 in comparison to 1985. Our results demonstrate the potential of a fuzzy set based approach to improve models of ice sheet hydrology in Western Greenland, by providing more reliable spatial distributions of entry points of melt water into the ice based on remotely sensed datasets of the ice surface, which are readily available.

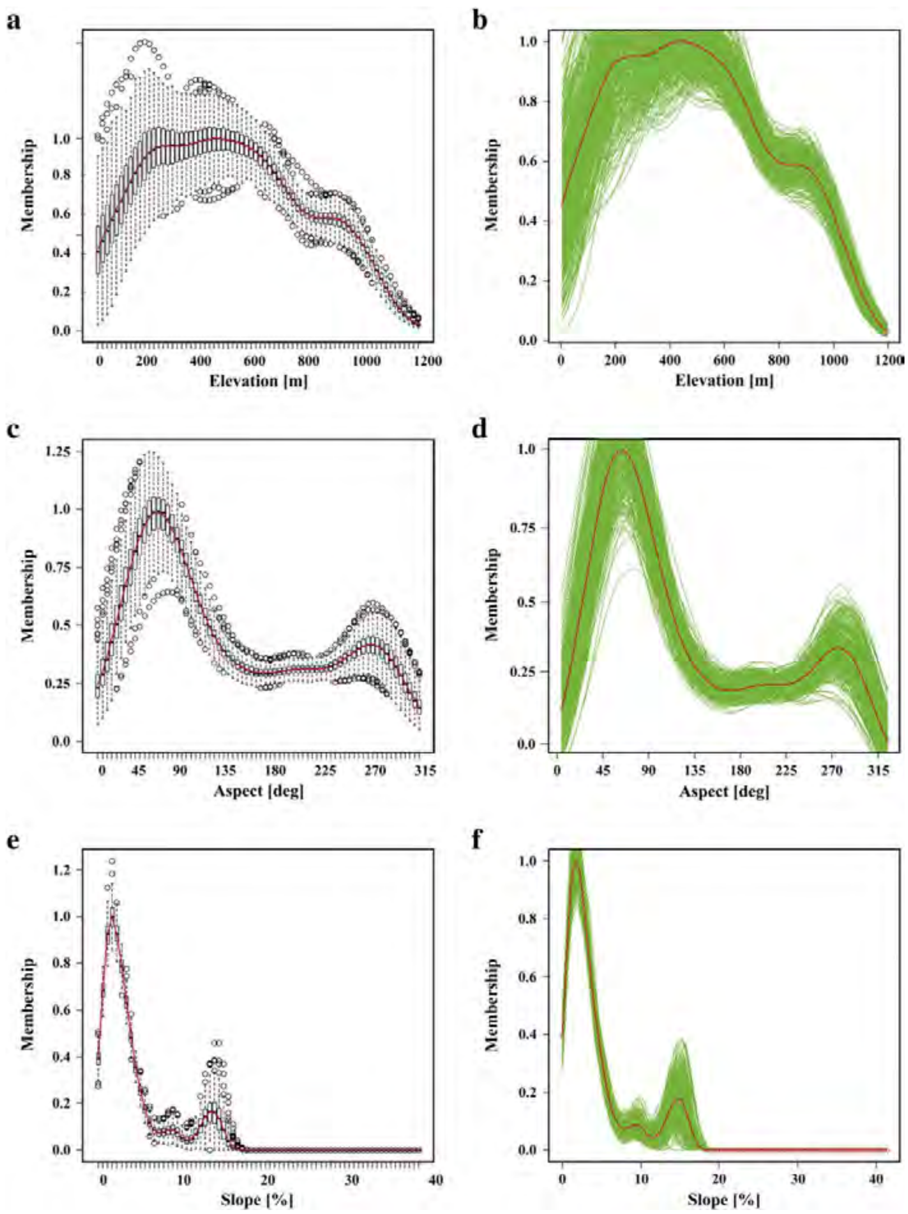

Figure 3.3.3: (Left): Box plots for the number of moulins/km2 as a function of elevation (a), aspect (c) and slope (e). (Right) Individual membership functions for all 500 Monte Carlo simulations (green) and their average (red), which was used as the membership function. The average membership functions were normalized in such a way that the minimum value was set to zero and the mean of the maximum was set to 1.

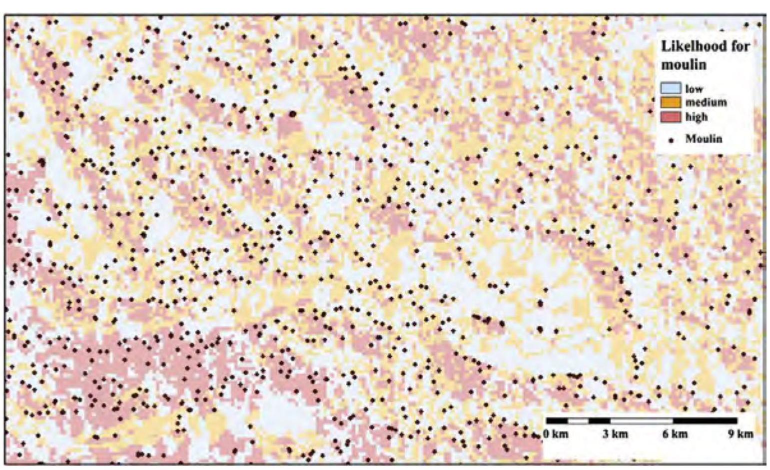

Figure 3.3.4: Blow up of the southern most regions showing the moulin likelihood and the moulin locations for 2008. Note that the extracted moulins seem to form at the upslope edges of medium and high likelihood areas.

3.3.3 Thermo-mechanical flowline model

Steady state thermo-mechanical flowline model to calculate the temperature profile and surface velocity of an ice sheet: (in preparation T. Phillips, H. Rajaram, L. Colgan and K. Steffen, Increased ice velocities due to cryo-hydrologic warming in Sermeq Avannarleq, west Greenland, *Nature Geoscience*).

The temperature and water content of ice have a large impact on its viscosity and hence on the deformational velocity of a glacier. The cross-sectional temperature profile of the Sermeq Avannarleq (SA) in Western Greenland is calculated using an enthalpy based steady-state 2D (xz) thermo-mechanical model. Using this model, we show that reasonable climb in the elevation of the equilibrium line, and hence an increase in the ablation zone area, results in an ice velocity increase of up to 70% due to changes in deformational velocity alone (Figure 3.3.5). In addition we are able to demonstrate that the basal sliding results in colder ice inflow that can potentially result in surface velocity decline due to the nonlinear relationship of ice temperature to its viscosity. The surface velocity of our model shows much agreement with observed surface velocities. We can also demonstrate that forcing current ice sheet models to flow at the observed surface velocity without including CHS but correcting by introducing basal slide, basic physical laws are violated: Basal velocities need to be introduced where a cold bed is expected, allowing enhanced amounts of cold ice to flow into usually warmer regions (Figure 3.3.6). We therefore believe that the inclusion of the CHS in future models is a necessity.

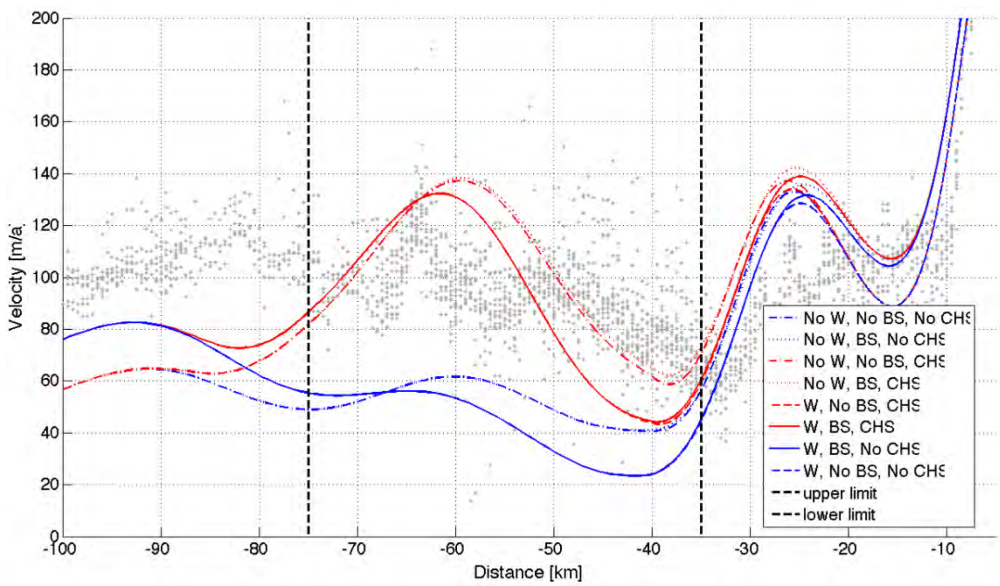

Figure 3.3.5: Comparison of surface velocity measurements (markers) with surface velocities predicted by coupled thermo-mechanical models. Red lines correspond to models where the warming influence of cryo-hydrologic warming was included in the energy equation, and blue lines correspond to models that did not include cryo-hydrologic warming. Different line styles in each category correspond to sensitivity studies involving other factors such as ice rheology and basal sliding. Across this range of model combinations, our results strongly suggest that the measured velocities in the region between -35 and -75 km from the terminus cannot be matched without considering the influence of cryo-hydrologic warming. Surface melt water generation has likely been occurring downstream of -45 km for the last few centuries. The region around -75 km began to receive surface melt around 2000. Currently melt is being detected as far as -95km. Due to contemporary climate warming; the upstream limit of surface melt water generation is likely to migrate farther upstream.

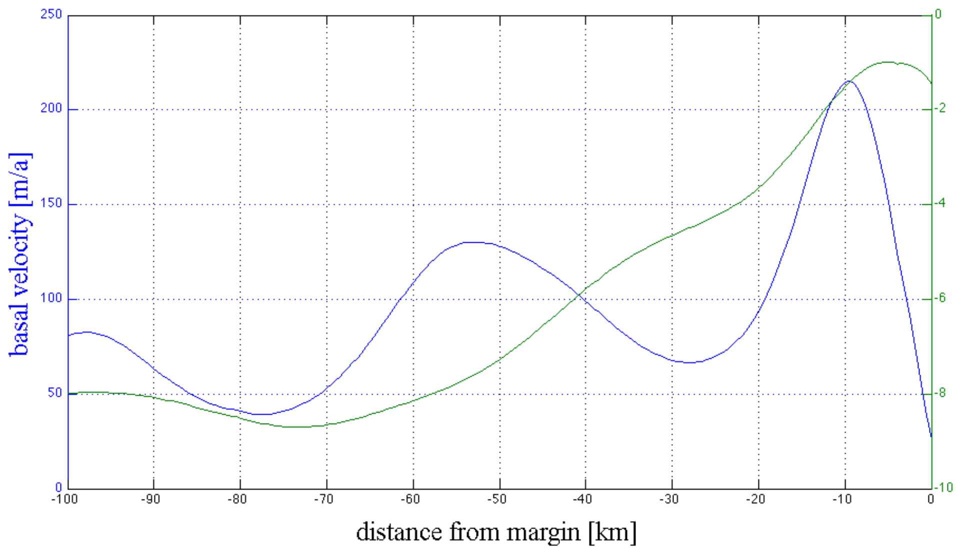

Figure 3.3.6: The basal velocity (blue) grows rapidly to unnaturally high velocities due to the stiffness of the overlying ice. In order to match the observed surface velocities basal slide has to be introduced in regions where the bed shows cold ice (green).

4. Proposed Field Activities and Research Objectives 2011

4.1 AWS Maintenance

The automatic weather station network will be maintained and upgraded. In the north, (GITS, Humboldt, Tunu-N, Petermann ELA, and NASA-SE new dataloggers (Campbell CR1000) will be installed. The new AWS at the UJS/EU drilling site (NEEM) will be maintained, and we plan to visit Summit. In the southern part of the ice sheet we will service the DYE-2, Saddle, NASA SE, Saddle, and S-Dome (Fig. 1.1), download the data and collect snow stratigraphy information.
The profile JAR2, JAR1, CU/ETH, and Crawford 1 will be serviced while at the Swiss Camp.

The field season 2011 will concentrate to upgrade AWS's on the Greenland ice sheet with updated data loggers and some new instrumentation. Further, we will install new GPS unites for those AWS's that transmit via GOES satellite and need a very accurate time stamp. Several AWS's have melted out in the ablation region near Swiss Camp and need to be re-drilled.

4.2 GPS Network Maintenance

Our effort to monitor the ablation along a transect from the Swiss Camp to the ice margin will continue. We will service the GPS network in collaboration with Dr. Jay Zwally (NASA-GSFC); in collaboration with Dr. Jose Rial (Duke University), we will install a seismic network at our main moulin location. We will continue to collect high-resolution surface topography data using Trimble Pathfinder differential GPS measurements along several transects in the lower ablation region. In addition, we will acquire ICEBRIDGE laser altimeter data to derive e a high resolution elevation model for the Jakobshavn ablation region in the vicinity of our AWS's.

4.3 Ground Penetration Radar

We have collected a number of ground penetrating radar (GPR) profiles along the western slope of the ice sheet (Jakobshavn and Kangerlussuaq region) in previous field seasons (1999, 2000, 2003, and 2007, 2008). The analysis of this data set showed that the accumulation could vary up to 40% between the trough and the ridge of the undulation. The surface topography with scale length of several kilometers plays an important role for the spatial variability of accumulation, the mass transfer, and the surface energy balance. We will repeat some of these GPR measurements during the spring 2010 field season along the same profiles to verify the recent accumulation changes and high percolation events in that region. We also purchased a new MALA 10 KHz ground penetrating antenna to map the underside of the Greenland ice sheet below Swiss Camp towards the ice margin in view of our moulin modeling. We will try to assess the sub glacial conduit density and the occurrence frequency of moulin (relics) in spring 2011.

5. Bibliography

Abdalati, W. and K. Steffen, 2001. Greenland ice sheet melt extent: 1979-1999, *J. Geophys. Res.,* 106(D24), 33,983-33,989.

Anderson, R., S. Anderson, K. MacGregor, E. Waddington, S. O'Neel, C. Riihimaki and M. Loso. 2004. Strong feedbacks between hydrology and sliding of a small alpine glacier. *J. Geophys. Res.* **109** (F03005), doi:10.1029/2004JF000120.

Bartholomaus, T., R. Anderson and S. Anderson. 2008. Response of glacier basal motion to transient water storage. *Nat. Geosci*. **1**: 33-37.

Bartholomew et al., 2010. Seasonal evolution of subglacial drainage and acceleration in a Greenland outlet glacier. *Nat. Geosci.* 3: 408-411. doi:10.1038/ngeo863.

Box, J., K. Steffen . 2001. Sublimation on the Greenland ice sheet from automated weather station observations. *J. Geophys. Res.* **106**(D24): 33,965-33,981.

Catania, and T. Neumann, 2010. Persistent englacial drainage features in the Greenland Ice Sheet. *Geophys. Res. Lett.* 37: doi:10.1029/2009GL041108.

Howat et al., 2008. Synchronous retreat and acceleration of southeast Greenland outlet glaciers 2000-2006: ice dynamics and coupling to climate. *J. Glaciol.* 54: 646-660.

Joughin, I., S. Das, M. King, B. Smith, I. Howat, T. Moon. 2009. Seasonal Speedup Along the Western Flank of the Greenland Ice Sheet. *Science* **320**.

Joughin, I., S. Das, M. King, B. Smith, I. Howat and T. Moon. 2008. Seasonal speedup along the western flank of the Greenland Ice Sheet. *Science*. **320**: 781-783.

Joughin et al., 2010. Greenland Flow Variability from Ice-Sheet-Wide Velocity Mapping. *J. Glaciol.* 56: 415-430.

Kamb, B., H. Engelhardt, M. Fahnestock and N. Humphrey. 1994. Mechanical and hydrologic basis for the rapid motion of a large tidewater glacier 2. Interpretation. *J. Geophys. Res.* **99**:

Marshall, S. 2005. Recent advances in understanding ice sheet dynamics. *Earth Plan. Sci. Lett.* **204**: 191-204.

Motyka et al., 2010. Volume change of Jakobshavn Isbrae, West Greenland: 1985–1997–2007. *J. Glaciol.* 56: 635-646.

Nghiem, S.V., K. Steffen, R. Kwok, and W.Y. Tsai. 2001. Diurnal variations of melt regions on the Greenland ice sheet, *J. Glaciol.,* 47(159), 539-547.

Nick et al., 2009. Large-scale changes in Greenland outlet glacier dynamics triggered at the terminus. *Nat. Geosci.* 2: doi:10.1038/ngeo394.

Pfeffer, 2007. A simple mechanism for irreversible tidewater glacier retreat. *J. Geophys. Res.* 112 (F03S25), doi:10.1029/2006JF000590.

Phillips et al., 2010. Cryo-hydrologic warming: A potential mechanism for rapid thermal response of ice sheets. *Geophys. Res. Lett.* 37: doi:10.1029/2010GL044397.

Price et al., 2008. Seasonal acceleration of inland ice via longitudinal coupling to marginal ice. *J. Glaciol.* 54: 213-219.

Rignot, E. and P. Kanagaratnam. 2006. Changes in the Velocity Structure of the Greenland Ice Sheet. *Science.* **311**: 986-990.

Shepherd et al., 2009. Greenland ice sheet motion coupled with daily melting in late summer. *Geophys. Res. Lett.* 36: doi:10.1029/2008GL035758.

Thomas, 2004. Force perturbation analysis of recent thinning and acceleration of Jakobshavn Isbrae, Greenland. *J. Glaciol.* 50: 57-66.

van den Broeke, M., J. Bamber, et al. 2009. Partitioning Recent Greenland Mass Loss. *Science* **326**(5955): 984-986.

van den Broeke et al., 2009. Partitioning Recent Greenland Mass Loss. *Science.* 326: doi:10.1126/science.1178176.

van der Veen, 1987. Longitudinal stresses and basal sliding: A comparative study. In: Dynamics of the West Antarctic Ice Sheet. Ed. C. van der Veen and J. Oerlemans.

van der Veen, 1998. Fracture mechanics approach to penetration of surface crevasses on glaciers. *Cold Reg. Sci. Tech.* 27: 31-47.

van der Veen et al., in press. Controls on the recent speed up of Jakobshavn Isbrae, West Greenland. *J. Glaciol.*

Zwally, H., W. Abdalati, T. Herring, K. Larson, J. Saba and K. Steffen. 2002. Surface melt-induced acceleration of Greenland Ice Sheet flow. *Science.* **297**: 218-222.